ABSTRACT

Modeling of Rapid Thermal Processing System by Finite Element Method

by
Helen Martynov

A finite element model for the Rapid Thermal Processing (RTP) system at NJIT was developed based on the software package MSC/NASTRAN. Based on this model, a thermal analysis of the 9" chamber, 3 zones (37 lamps) RTP system was conducted for various modes of system operation with the 6" silicon wafer temperature varying from 300°K to 1100°K. An open-loop control algorithm was developed in order to study the dependance of wafer temperature on time, position, and applied radiant heat distribution. It was shown that the non-uniformity in the radial temperature profile can be less than 3°C during wafer heating at the rate of 35°C per second.

The developed model was also utilized for the analysis of the change in the wafer temperature profile due to the heat loss through thermocouple wiring attached to the wafer. It was shown that for a 0.005" Nickel-Chromium thermocouple the maximum disturbance of the wafer temperature profile at the thermocouple contact was only of the order of 0.1°C with the wafer temperature in the interval from 800°K to 1100°K.

MODELING OF RAPID THERMAL PROCESSING SYSTEM
BY FINITE ELEMENT METHOD

by
Helen Martynov

A Thesis
Submitted to the Faculty of the
New Jersey Institute of Technology
in Partial Fulfillment of the Requirements for the Degree of
Master of Science in Electrical Engineering

Department of Electrical and Computer Engineering
October 1993

Blank Page

APPROVAL PAGE

Modeling of Rapid Thermal Processing System by Finite Element Method

Helen Martynov

8/25/93

Dr. Walter F. Kosonocky, Thesis Advisor
Distinguished Professor of Electrical and Computer Engineering,
NJIT Foundation Chair for Optoelectronics and Solid State Circuits

8/25/93

Dr. Constantine N. Manikopoulos, Committee Member
Associate Professor of Electrical and Computer Engineering, NJIT

8/25/93

Dr. Edwin Hou, Committee Member
Assistant Professor of Electrical and Computer Engineering, NJIT

BIOGRAPHICAL SKETCH

Author: Helen Martynov

Degree: Master of Science in Electrical Engineering

Date: October 1993

Date of Birth:

Place of Birth:

Undergraduate and Graduate Education:

- Master of Science in Electrical Engineering,
  New Jersey Institute of Technology, Newark, NJ, 1993

- Master of Science in Applied Mathematics,
  Moscow Power Engineering Institute, Moscow, USSR, 1989

Major: Electrical Engineering

This thesis is dedicated to
my Mother

ACKNOWLEDGMENT

TABLE OF CONTENTS

LIST OF TABLES

LIST OF FIGURES

CHAPTER 1

INTRODUCTION

The research work reported in this thesis represents theoretical analysis performed in support of the effort of Electronic Imaging Center of the NJIT Foundation for Optoelectronics and Solid-State Circuits under ARPA contract F33615-92-C-5817 "Multi-Wavelength Imaging Pyrometry for Semiconductor Process Monitoring and Control". This work was done under the general direction of Professor Walter F. Kosonocky.

The objective of this work included the development of a finite element model for Rapid Thermal Processing (RTP) system and thermal analysis of RTP under various process conditions. In addition, the utilization of the finite element model for a real-time control algorithm is considered in this work.

Chapter 2 provides a brief description of the theoretical concepts utilized in this work. The structure of the RTP system is briefly described in the first section of this chapter. The second section of this chapter introduces the basic concepts of heat transfer analysis. The third section provides the overview of the underlying ideas of the finite element method (FEM).

Chapter 3 provides a detailed description of the finite element model for the RTP system. The overview of the general structure and capabilities

of the finite element based software package MSC/NASTRAN is given at the beginning of the chapter. The geometry of the finite element model of RTP system along with the selected discretization (mesh) of the system components into finite elements is described in the second section of this chapter. The chapter concludes with a description of the algorithm utilized for modeling of semitransparent quartz window, which had to be developed in order to circumvent the inability of MSC/NASTRAN to simulate the semitransparent bodies.

Chapter 4 describes the transformation of view factors computed by MSC/NASTRAN into generalized radiation exchange coefficients appropriate for real time control software. The first section of this chapter provides a brief description of the generalized model of the RTP system developed at the NJIT Electronic Imaging Center for the purpose of real time control algorithm. The major differences between finite element and generalized models are discussed. The second section provides the actual algorithm for transformation of view factors generated by MSC/NASTRAN to the generalized radiation exchange coefficients appropriate for real time control. This procedure allows the real time control algorithm to utilize the accurate information about the radiometric characteristics of the RTP system, thus avoiding the computationally expensive calculations performed by MSC/NASTRAN.

The discussion of the simulation results is given in Chapter 5. The calibration of the developed finite element model against the experimental data is discussed at the beginning of the chapter. The second section of this chapter provides the analysis of the wafer temperature profiles obtained by simulation of RTP operation under various process conditions. This chapter concludes with the simulation-based analysis of the disturbance of wafer temperature profile introduced by attached to the wafer surface thermocouple.

Chapter 6 presents a summary and the conclusions of this thesis work.

CHAPTER 2

BASIC THEORETICAL CONCEPTS

2.1 Rapid Thermal Processing (RTP)

Rapid thermal processing is a relatively new technology used in processing of semiconductor wafers for manufacture of integrated circuits. At the present time RTP is applied to a variety of thermal processing steps including dopant activation and grain growth of polycrystalline silicon, formation of silicides, contact formation, growth of thin oxides and nitrides, epitaxial silicon deposition, as well as a fabrication of the variety of devices [1].

A simplified schematic of RTP system is shown in Figure 1. In RTP the wafer is heated by the infrared radiation of tungsten-halogen lamps positioned above the quartz window of the reaction chamber. In the RTP system considered in this thesis the tungsten-halogen lamps are arranged in three annual zones consisting of 1, 12 and 24 lamps. The central lamp zone consists of one 2kW lamp, the remaining two zones consist of 1kW lamps. The distance between the first, second and third zones of lamps and quartz window are 0.56", 2.13" and 1.25" respectively as illustrated in Figure 1. The electrical power supplied to each zone of lamps can be controlled independently, however, there is no provision for adjustment of power levels supplied to the individual lamps.

4
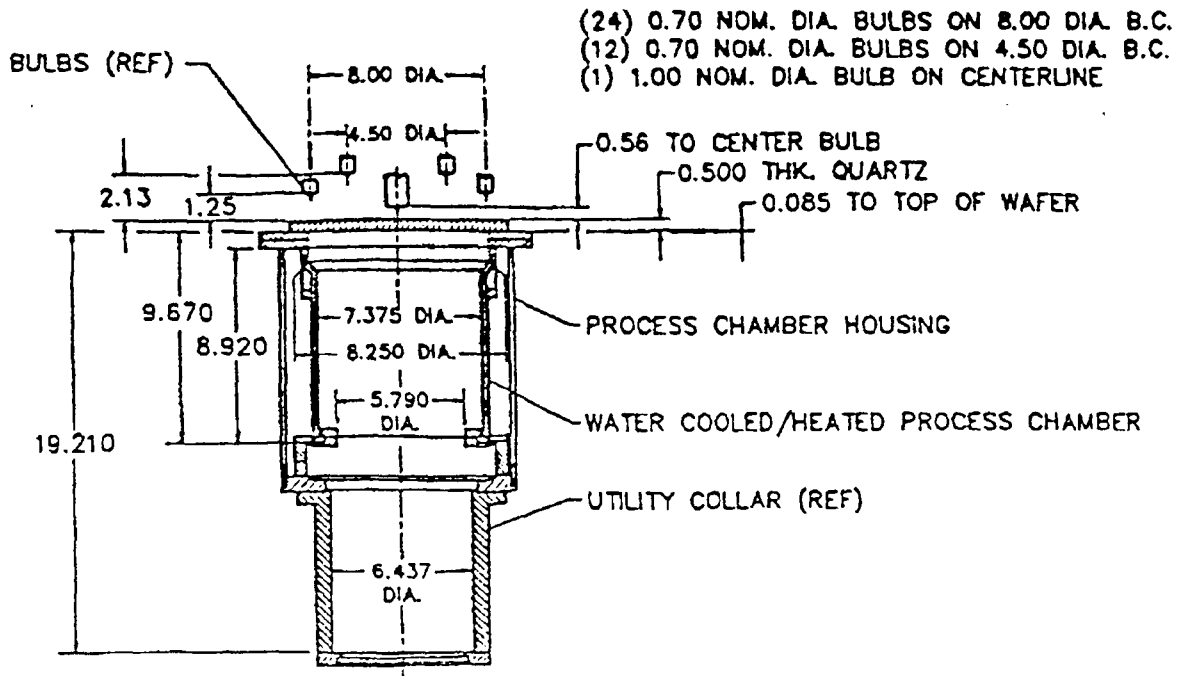
Figure 1. A simplified schematic of RTP system.

The semiconductor wafer (assumed to be silicon wafer for the purpose of present analysis) is positioned 0.085" below quartz window and is supported by three - pin wafer holder. The walls of the RTP chamber are made from stainless steel and are water-cooled, thus having constant temperature of approximately 300K. The quartz window at the top of the RTP chamber is water-cooled at the edges. In addition, the quartz is being cooled by the room temperature air blown on its top surface.

The ambient in the process chamber may be vacuum or a process gas depending on the thermal process being performed. The temperature of the wafer is continuously monitored by the infrared pyrometer positioned above the quartz window [1] or by IR imager through the sapphire window at the bottom of the RTP chamber [2]. In addition, for calibration of the IR detectors, the temperature of the instrumented wafer may be measured by the attached to the wafer surface K-type thermocouples [3]. The information about wafer temperature is then fed back to the real time control algorithm which controls the power supplied to each lamp zone.

During thermal processing of semiconductor wafers it is very important that the wafer temperature follows a prescribed temperature trajectory and that the temperature profile across the wafer is uniform [4]. In order to achieve this goal the accurate thermal model of RTP system should be supplied to the real time algorithm controlling the input power to the tungsten-halogen lamps. One of the major objectives of this work is to build the adequate thermal model of the RTP system based on the detailed heat transfer analysis.

2.2 Basic Concepts of Heat Transfer Analysis

The basic equation of heat transfer is based on the law of conservation of energy. The heat transfer analysis of any system requires the solution of the following energy balance equation:

$$\dot{E}_{in} + \dot{E}_g = \dot{E}_{out} + \dot{E}_{ie} \qquad (2\text{-}1)$$

where

$\dot{E}_{in}$ - is the rate of energy inflow into the system,

$\dot{E}_g$ - is the rate of energy generated inside the system,

$\dot{E}_{out}$ - is the rate of energy outflow from the system,

$\dot{E}_{ie}$ - is the rate of change in internal energy of the system.

The energy generated in a solid body may be due to chemical, nuclear or electromagnetic energy which is converted into thermal energy. Its rate is governed by the equation:

$$\dot{E}_g = q\,V \qquad (2\text{-}2)$$

where

q - is the rate of energy per unit volume, per unit time generated by internal heat source,

V - is a volume of solid body.

The rate of energy stored in a solid body is described by equation

$$\dot{E}_s = \rho C \frac{\partial T}{\partial t} \tag{2-3}$$

where

ρ - is the density of material,

C - is the specific heat of material.

The rate equations which describe the rates of energy flows are obtained from laws of three basic modes of heat transfer: conduction, convection and radiation.

Heat conduction is the transfer of heat through material either by interaction of molecules with different energy levels or by motion of free electrons. The rate of heat flow by conduction (per unit area) is described by Fourier law:

$$q = -k\nabla T \tag{2-4}$$

where

$q = \begin{Bmatrix} q_x \\ q_y \\ q_z \end{Bmatrix}$ is a vector in Casterian coordinates,

$\nabla = \frac{\partial}{\partial x} i + \frac{\partial}{\partial y} j + \frac{\partial}{\partial z} k$, where i,j,k is the basis of the coordinate system.

Convection is a mode of heat transfer which involves the heat exchange between surface of a solid body and fluid or gas surrounding it, Its rate is represented by Newton rate equation:

$$q = hA(T_{surf} - T_\infty) \qquad (2\text{-}5)$$

where

h - is the heat transfer coefficient,

T_{surf} - is the temperature of the body surface,

T_∞ - is the temperature of surrounding medium.

Heat transfer by radiation can be considered as an electromagnetic phenomenon and defined as the transfer of energy between two surfaces (or the surface and the medium) via electromagnetic waves with no physical media required for propagation. The amount of radiation per wavelength interval may vary with wavelength and is characterized by spectral distribution. The preferential emission in certain direction and its dependence on position across a surface characterize a directional and positional distributions respectively.

To describe the radiation characteristics of real surfaces it is useful to introduce the concept of the blackbody. The blackbody is an idealization based on the response to incident thermal radiation with the following properties:

(1) A blackbody absorbs all incident radiation, regardless of wavelength and direction.

(2) For a given temperature and wavelength, no surface can emit more thermal radiation than a blackbody.

(3) The radiation emitted by a blackbody is independent of direction.

The value of the total radiant power emitted from a unit of blackbody surface area over the wavelength range from zero to infinity known as Stefan-Boltzmann law, can be expressed as

$$L_{0\to\infty,b} = \sigma \cdot T^4 \qquad (2\text{-}6)$$

where $\sigma = 5.67 \times 10^{-8} \, [\text{W} / \text{m}^2 \cdot \text{K}^4]$ - is the Boltzmann constant.

The behavior of real surfaces is described by four radiative properties coefficients: emissivity (ε), absorptivity (α), reflectivity (ρ) and transmissivity (τ). Emissivity is defined as a ratio of the radiation emitted by a surface under consideration to the radiation emitted by a blackbody at the sane temperature and for the same spectral and directional conditions.

$$\varepsilon(\lambda,\theta,T) = \frac{L_{\lambda,em}(\lambda,\theta,T)}{L_{\lambda,b}(\lambda,T)} \qquad (2\text{-}7)$$

The portions of absorbed, reflected and transmitted radiation to incident radiation define absorptivity, reflectivity and transmissivity respectively.

The radiation balance requires that

$$\alpha(\lambda,\theta,T) + \rho(\lambda,\theta,T) + \tau(\lambda,\theta,T) = 1 \qquad (2\text{-}8)$$

The approximations of radiative surfaces as gray and diffusive yield independent from wavelength and direction radiative coefficients which simplify the radiative heat transfer analysis considerably. This approximation is employed in this work for the purpose of finite element modeling.

When the system consists of more than one surface the radiant energy exchange between the surfaces depends not only on radiative properties of the surfaces but on geometry of the system as well. The concept of view factor provides the base for analysis of radiation exchange.

View factor between two surfaces defines the portion of energy that leaves one surface and is incident on another. To evaluate the view factor, consider the radiation exchange between two small surfaces dA_l and dA_m ,which are located on A_l and A_m respectively. The view factor $df_{l\to m}$ between Lambertian surfaces dA_l and dA_m is given by

$$df_{l\to m} = \frac{\cos(\theta_l)\cos(\theta_m)}{\pi r_{l\leftrightarrow m}^2} \qquad (2\text{-}9)$$

where (as shown in Figure 2 [5])

r_{l-m} - is the length of the line connecting dA_l and dA_m,

θ_l and θ_m - are the angles between the connecting line and the normals to the surfaces l and m.
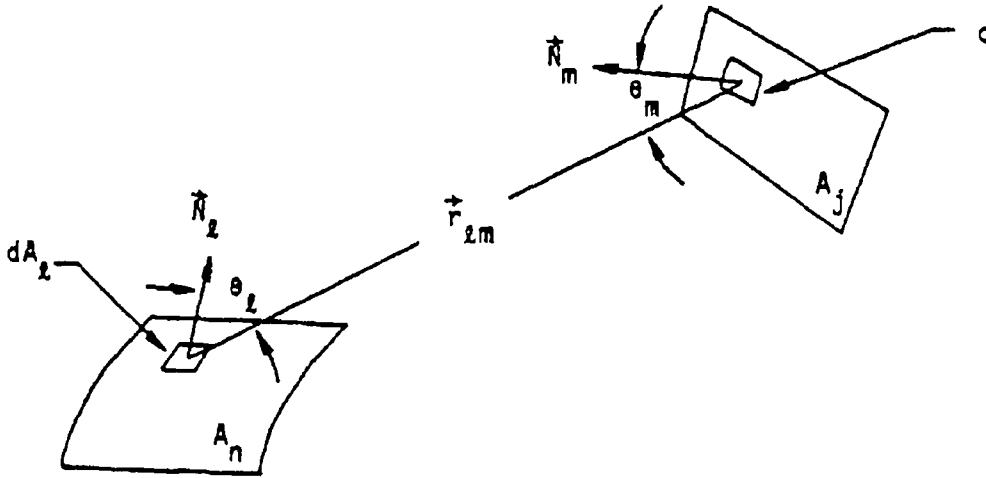
Figure 2. View factor notation [5]

The view factor between surfaces l and m is determined by integration of Equation (2-9) over both surfaces:

$$f_{l \to m} = \frac{1}{A_l} \int_{A_m} \int_{A_l} \frac{\cos(\theta_l)\cos(\theta_m)}{\pi r_{l \leftrightarrow m}^2} dA_l dA_m \qquad (2\text{-}10)$$

The reciprocity theorem [6] states that

$$F_{l \to m} = A_l f_{l \to m} = A_m f_{m \to l} = F_{m \to l} \qquad (2\text{-}11)$$

Combining all previous equations together, the following governing differential equation for heat transfer is obtained:

$$\frac{\partial}{\partial x}(k_x \frac{\partial T}{\partial x}) + \frac{\partial}{\partial y}(k_y \frac{\partial T}{\partial y}) + \frac{\partial}{\partial z}(k_z \frac{\partial T}{\partial z}) + \dot{q} = \rho C \frac{\partial T}{\partial t} \qquad (2\text{-}14)$$

Subject to possible boundary and initial conditions:

- prescribed surface temperature T_p :

$$T_s(x,y,z,t) = T_p \qquad (2\text{-}15)$$

- prescribed surface heat flux q_p :

$$q_x n_x + q_y n_y + q_z n_z = -q_p \qquad (2\text{-}16)$$

where

n_x, n_y, n_z - direction cosines of outward normal to the surface

- convective heat loss from surface :

$$q_x n_x + q_y n_y + q_z n_z = h(T_s - T_\infty) \qquad (2\text{-}17)$$

- radiation heat loss from surface:

$$q_x n_x + q_y n_y + q_z n_z = \sigma \varepsilon T_s^4 - \alpha q_s^{in} \qquad (2\text{-}18)$$

- initial temperature profile:

$$T(x,y,z,t=0) = T_0(x,y,z) \qquad (2\text{-}19)$$

2.3 Basic Concepts of Finite Element Method (FEM)

The existing mathematical tools are not sufficient to find the exact solution of Eq. (2-14) with conditions (2-15) - (2-19) within a complex system. Therefore, the approximate numerical solution to the problem had to be found. One of the most powerful and advanced numerical methods for solution of partial differential equations within complex geometry is FEM.

The idea of FEM goes back to R. Courant who proposed in 1943 [7] the method to solve continuum problem by breaking the solution domain into triangular regions and replacing the unknown variable (often called field in engineering applications of FEM) by piecewise approximation within each triangle.

The solution of general continuum problem by FEM is converted to solution of the system of algebraic equations always following orderly step by step process:

(1). Discretization of the domain

The first step is to divide the structure into finite elements connected with each other in node points. The number, type and size of the elements have to be decided.

(2). Selection of proper interpolation functions

The solution within an element is approximated by a simple function that satisfies the convergence and continuity requirements, generally polynomial.

(3). Derivation of element properties

Based on assumed model the matrix equations expressing element properties and element characteristic matrices (stiffness matrix, load vector) are determined by direct, variational or weighted residual approaches.

(4). Assemblage of element equations to obtain system equations

Matrix equations for each element are combined to the bigger system of equations of the same form.

(5). Solution for the unknown field variable

The resulted system of simultaneous equations can always be solved using known techniques for solving the system of algebraic equations.

(6). Additional computations of system parameters if desired.

If the variation for field variable Φ is assumed to be polynomial then Φ can be expressed as:

$$\Phi(x,y,z) = \alpha_1 + \alpha_2 x + \alpha_3 y + \alpha_4 z + \alpha_5 xy + \alpha_6 x^2 + ... + \alpha_m z^n \qquad (2\text{-}20)$$

or in vector notation [8]

$$\Phi(x,y,z) = \eta^T \alpha \qquad (2\text{-}21)$$

where

$$\eta^T = \{1 \quad x \quad y \quad z \quad xy \quad x^2 ... z^n\}$$

$$\alpha = \begin{Bmatrix} \alpha_1 \\ \bullet \bullet \bullet \\ \alpha_m \end{Bmatrix} \text{ is the vector of coefficients of the polynomial of Eq.(2-20)}$$

For typical finite element **e** with **M** nodes the approximating polynomial for field variable Φ can be expressed in terms of values of field variable in its nodes. Evaluation of η^T at nodal coordinates $(\bar{\eta})$ and substitution $\bar{\eta}$ into Eq. (2-21) gives

$$\begin{Bmatrix} \Phi(\text{at node } 1) \\ \bullet \bullet \bullet \\ \Phi(\text{at node } M) \end{Bmatrix} = \Phi^{(e)} = \begin{bmatrix} \bar{\eta}(\text{at node } 1) \\ \bullet \bullet \bullet \\ \bar{\eta}(\text{at node } M) \end{bmatrix} \alpha = [\tilde{\eta}]\alpha \qquad (2\text{-}22)$$

where

$\Phi^{(e)}$ - is a vector of nodal values of field variable Φ,

$$[\tilde{\eta}] = \begin{bmatrix} \bar{\eta}(\text{at node } 1) \\ \bullet \bullet \bullet \\ \bar{\eta}(\text{at node } M) \end{bmatrix} \text{is a square matrix of vectors.} \eta^T \text{evaluated at nodal}$$

coordinates.

Then:
$$\alpha = [\tilde{\eta}]^{-1} \Phi^{(e)} \qquad (2\text{-}23)$$

Substitution Eq. (2-23) into Eq.(2-21) gives the interpolation value of field variable Φ inside the element in terms of nodal values of the field $\Phi^{(e)}$ as:

$$\Phi = \eta^T [\tilde{\eta}]^{-1} \Phi^{(e)} = [N]\Phi^{(e)} \qquad (2\text{-}24)$$

where

$[N] = \eta^T [\tilde{\eta}]^{-1}$ - is a set of interpolation functions.

For each element the interpolation functions N_j can be expressed in terms of local coordinate system specific to each element by using coordinate transformation relations.

As was already mentioned, in order to derive element equations several approaches can be used. Most of the continuum problems may have either differential or variational formulation. In differential formulation the problem is to integrate a differential equation or system of differential equations subject to given boundary conditions. In variational formulation the problem is to make stationary (usually to minimize) functional or system of functionals, subject to the same boundary conditions.

It can be shown, that the problem formulations are equivalent because the functions which satisfy the differential equations also make the functional stationary.[8]

Let us give the brief overview of variational approach.

Consider the general functional I:

$$I = \iiint_V F[\Phi,\Phi_x,\Phi_y,\Phi_z,\Phi_{xy}...]dV + \iint_S g[\Phi,\Phi_x,\Phi_y,\Phi_z,\Phi_{xy}...]dS \quad (2\text{-}25)$$

where Φ is unknown field variable and the subscripts denote the partial derivative with respect to coordinates.

To make functional stationary with respect to nodal unknowns Φ_i, the following condition has to be satisfied:

$$\left\{ \begin{array}{c} \partial I/\partial \Phi_1 \\ \bullet \ \bullet \ \bullet \\ \partial I/\partial \Phi_N \end{array} \right\} = 0 \qquad (2\text{-}26)$$

where N - total number of nodal unknowns in the system.

The Eq.(2-26) leads to the final system of linear equations that can be solved by commercially available software. In the next chapter the derivation of algebraic system of equations based on variational formulation will be considered for RTP system.

CHAPTER 3

FINITE ELEMENT MODEL OF RTP SYSTEM

3.1 Finite Element Based MSC/NASTRAN Software Package

First implementations of FEM for solving engineering problems by means of software products were made mostly in aircraft industry, including NASA project that led to NASTRAN (NASA STRuctural ANalysis). At the present time MSC/NASTRAN is available as a commercial software marketed by MacNeal - Schwendler Corporation. The capabilities of MSC/NASTRAN include structural, heat transfer, acoustic, electromagnetic modes of analysis.

MSC/NASTRAN is capable of analyzing linear and nonlinear heat transfer problems in both steady-state and transient modes. The modeling capabilities include the simulation of temperature dependent properties of material as well as wide variety of boundary conditions. In addition, MSC/NASTRAN provides extensive graphical capabilities for model generation and result analysis.

The finite element model is formed by subdividing the simulated structure into limited number of finite elements. These elements are connected to each other at nodal points called grid points. The dimension of element may vary from 0D to 3D. The orientation of coordinate system,

locations of grid points and their connectivities define the geometry of the model.

The mechanism by which model interacts with its surroundings such as enforced temperatures, surface and volumetric loads and radiation effects are modeled by heat boundary elements, HBDY, that overlay the surfaces of finite elements on the boundaries.

Material properties such as thermal conductivity, specific heat, emissivity and absorptivity are assigned to each element independently, thus providing the capability to model the positional variations of these properties.

Described above types of input data form the Bulk Data deck which defines the finite element model. The solution flow is controlled by Executive deck, while Case Control deck controls the output and selects input data from alternative sets. The output from MSC/NASTRAN may include temperature at grid points, interelement heat fluxes and heat balance data in terms of applied loads, constraints and temperature derivatives.

The general equation solved by MSC/NASTRAN for heat transfer problem is given by [5]

$$[K]\{u\} + [B]\{\dot{u}\} = \{P\} + \{N\} \qquad (3\text{-}1)$$

where

$\{u\}$ - is a vector of temperatures at grid points,

$\{\dot{u}\}$ - is a vector of temperature gradients at grid points

$\{P\}$ - is a vector of applied heat fluxes that are known functions of time

$\{N\}$ - is a vector of nonlinear heat fluxes as a function of temperature

$[K]$ - is a symmetric matrix of constant heat conduction coefficients

$[B]$ - is a symmetric matrix of constant heat capacity coefficients

The temperatures of all elements are related through a set of simultaneous algebraic equations written in terms of grid points. MSC/NASTRAN assembles and solves these equations for temperature distribution. Heat flows are calculated by subsequent data recovery operations. The simplified solution flow diagram is shown in Figure 3.[5]

```
                    ┌─────────────────────────┐
                    │   Input File Processor   │
                    └─────────────────────────┘
                                 │
                                 ▼
                    ┌─────────────────────────┐
                    │   Geometry Processor     │
                    └─────────────────────────┘
                                 │
                                 ▼
                    ┌─────────────────────────┐
                    │    Structure Plotter     │
                    └─────────────────────────┘
                                 │
                                 ▼
                   ┌────────────────────────────┐
                   │  Conduction and Capacity   │
                   │     Matrix Assembly        │
                   └────────────────────────────┘
                                 │
                                 ▼
                  ┌──────────────────────────────┐
                  │ Generate Radiation Matrix,    │
                  │   Combine with Conduction     │
                  │          Matrix               │
                  └──────────────────────────────┘
                                 │
                                 ▼
               ┌───────────────────────────────────┐
               │ Apply Constraints, Partition      │
               │            Matrices               │
               └───────────────────────────────────┘
                                 │
                                 ▼
                  ┌──────────────────────────────┐
                  │  Dynamic Pool Distributor     │
                  └──────────────────────────────┘
                                 │
                                 ▼
                    ┌─────────────────────────┐
                    │   Direct Matrix Input    │
                    └─────────────────────────┘
                                 │
                                 ▼
                  ┌──────────────────────────────┐
                  │  Assemble Dynamic Matrices    │
                  └──────────────────────────────┘
                                 │
                                 ▼
                  ┌──────────────────────────────┐
                  │  Transient Load Generator     │
                  └──────────────────────────────┘
                                 │
                                 ▼
                 ┌────────────────────────────────┐
                 │ Integration of Equations, with │
                 │  Nonlinear Loads and Radiation │
                 └────────────────────────────────┘
                                 │
                                 ▼
                   ┌────────────────────────────┐
                   │   Output Solution Points    │
                   └────────────────────────────┘
                                 │
                                 ▼
                 ┌────────────────────────────────┐
                 │ Recover Dependent Temperatures │
                 │   and Element Fluxes           │
                 └────────────────────────────────┘
                                 │
                                 ▼
                       ┌──────────────────┐
                       │     X-Y Plot      │
                       └──────────────────┘
                                 │
                                 ▼
                    ┌─────────────────────────┐
                    │    Structure Plotter     │
                    └─────────────────────────┘
```
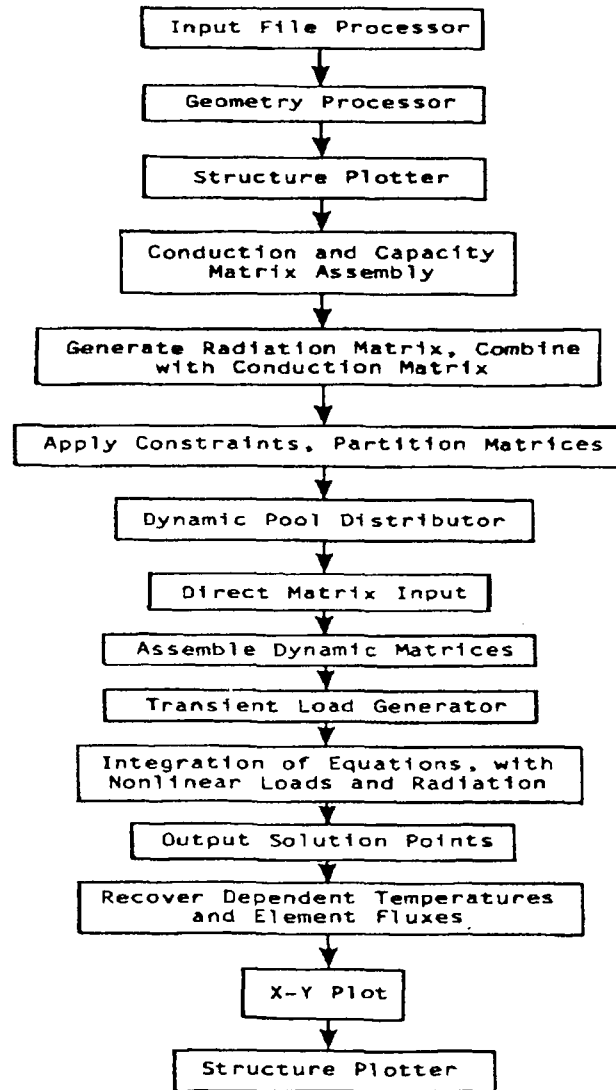
Figure 3. Solution flow diagram for general heat transfer problem [5]

3.2 Geometry of the Finite Element Model of RTP System

The first step in building the finite element model for MSC/NASTRAN involves the subdivision of modeled system into finite elements. The optimal discretization depends on the geometrical configuration of the

particular system, required accuracy of the solution, and the type of boundary conditions.

In the case of MSC/NASTRAN the subdivision of the model into elements, or mesh, is the responsibility of the user. The principal concerns in making the selection between the finer and coarser mesh are the accuracy and utilization of computer resources, both of which increase with the increasing number of elements in the model. The finite elements for RTP model were selected based on the above considerations from the element types supported by MSC/NASTRAN. The two-dimensional finite elements supported by MSC/NASTRAN include triangular element (TRIA) and quadrilateral element (QUAD). QUAD elements are assumed to be composed from two or four triangles. Three types of three-dimensional finite elements most commonly used for heat transfer analysis are tetrahedron (TETRA), pentahedron (PENTA) and hexahedron (HEXA). Tetrahedron is similar to a pyramid, except all four of its sides are triangles. Pentahedron is five-sided element with six vertices, or grid points. The hexahedron is a six-sided element with eight grid points and quadrilaterial sides. The sizes and shapes of these elements are arbitrary, but the accuracy may be reduced if triangular sides of pentahedron or opposite sides of hexahedron are not parallel within about 30° [9].

Within each element the temperature is expressed as a polynomial function of temperatures in element grid points. The complexity of this

approximating polynomial depends on the number of grid points associated with element. In case of TETRA and TRIA elements, the temperature field within the element is approximated by linear combination of temperatures at grid points. As a result of this linearization, the better accuracy of the solution corresponds to increased density of finite elements in the regions with high temperature gradients.

For the purpose of heat transfer analysis four major components of RTP system were subdivided into finite elements as follows:

1. The 6" silicon wafer was subdivided into 132 finite elements which can be grouped into 11 rings and 12 sectors as shown in Fig. 4. Due to the fact that central halogen lamp is positioned most closely to the wafer surface the temperature gradients in the central part of the wafer were expected to be higher. Accordingly, the central part of the wafer was subdivided into ring of 12 relatively small PENTA elements. The remaining part of the wafer was subdivided into 10 rings consisting of 12 HEXA elements each, with dimensions of the HEXA elements increasing toward the edge of the wafer. The thickness of all elements comprising the model of the wafer was taken to be 0.025".

2. The quartz window on the top of the RTP chamber was subdivided into 10 PENTA elements, each having a common point at the center of the window, as shown in Fig. 5. The thickness of all PENTA elements was taken to be 0.5".
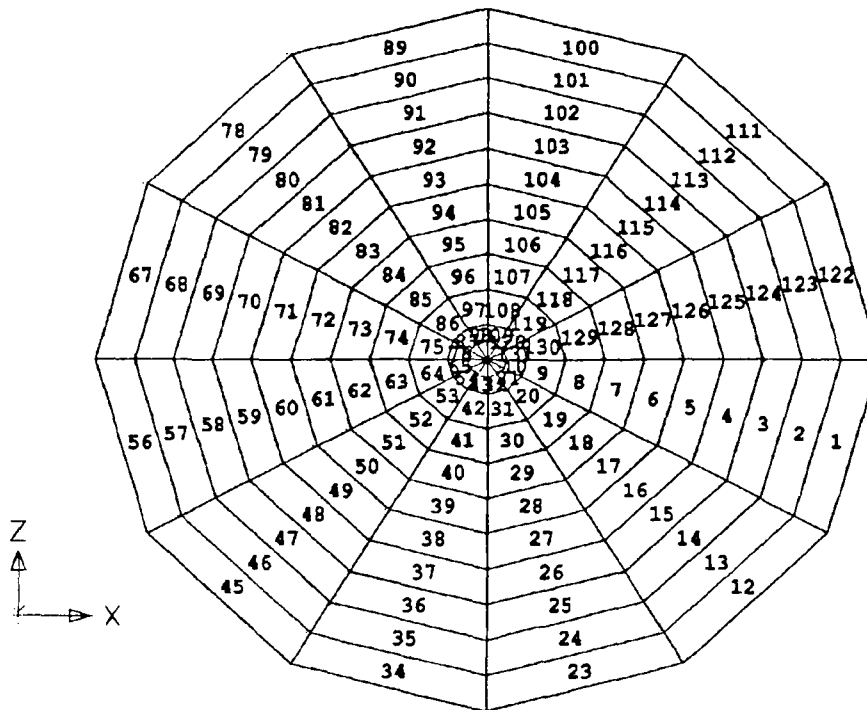
Figure 4. The silicon wafer mesh

3. The RTP chamber was subdivided into 30 two-dimensional elements. The vertical walls of the chamber were divided into 10 QUAD elements of equal size. The bottom of the chamber was divided into 10 TRIA elements and 10 QUAD elements positioned into 2 rings of 10 elements each. The inner ring consists of 10 TRIA elements which allow for simulation of the sapphire window at the bottom of the RTP chamber.

4. The tungsten-halogen lamps were modeled as point elements (POINT) grouped into three rings with one, twelve, and twenty four lamps respectively. The diameter of the inner lamp was taken to be 1", all other lamps have the diameter of 0.7"

The described above model geometry is illustrated in Figures 5 and 6.
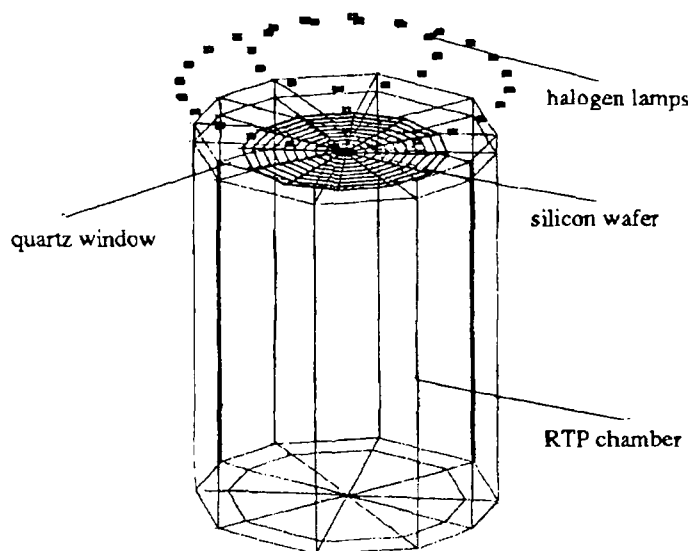

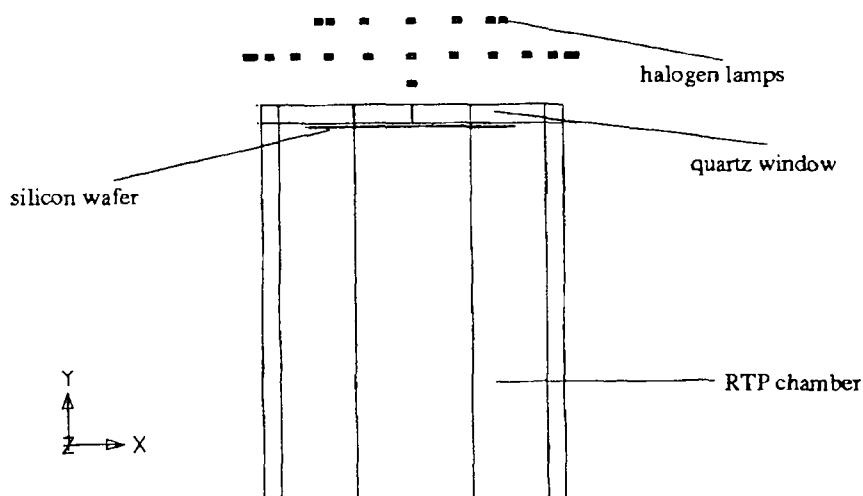**Figure 5.** The geometry of the model of RTP system

Figure 6. The front view of the model.

At this point it should be noted that the described above subdivision of the RTP system components into finite elements was obtained by a series of computational experiments. At first, a very coarse mesh was selected for all components of the model and the resulting temperature field was

computed. Next, the mesh for each model component was refined, increasing the number of finite elements by a factor of 2. The temperature profile computed with the new mesh was compared against the results obtained on the previous iteration and so on. The final mesh described above was selected because the further refinement of the mesh by a factor of 2 produced the difference in the wafer temperature profile of less than 0.1%. Therefore, the further increase in the complexity and computational cost of the model was deemed unnecessary.

3.3 Heat Transfer within the Model of RTP System

Our main interest in heat transfer analysis of RTP system is to find the temperature distribution across the silicon wafer. The materials comprising the RTP system components are assumed to be isotropic and their thermal properties are assumed to be independent of temperature. In other words, the thermal properties of the components of RTP system are presumed to be constant within each system component.

All three basic modes of heat transfer are present in the analysis. The quartz window is air-cooled, therefore the heat transfer by convection is modeled between top surface of the quartz window and the air with temperature of 300K. Radiation heat exchange is considered between all components of RTP system. All water-cooled components of RTP chamber

are assumed to have constant temperature of 300K. No volumetric heat generation is present within the system.

Our goal is to find a solution of heat balance Eq. (2-14) which in our case can be expressed for each component of the RTP system as:

$$\frac{\partial}{\partial x}(k_x \frac{\partial T}{\partial x}) + \frac{\partial}{\partial y}(k_y \frac{\partial T}{\partial y}) + \frac{\partial}{\partial z}(k_z \frac{\partial T}{\partial z}) = \rho C \frac{\partial T}{\partial t} \qquad (3\text{-}2)$$

where the following boundary and initial conditions should be satisfied:

- prescribed temperature T_p =300K on chamber surface:

$$T_s(x,y,z,t) = T_p \qquad (3\text{-}3)$$

- convective heat loss from top quartz surface :

$$q_x n_x + q_y n_y + q_z n_z = h(T_s - 300) \qquad (3\text{-}4)$$

- radiation heat loss from all surfaces:

$$q_x n_x + q_y n_y + q_z n_z = \sigma \varepsilon T_s^4 - \alpha q_s^{in} \qquad (3\text{-}5)$$

- initial temperature profile:

$$T(x,y,z,t=0) = T_0(x,y,z) \qquad (3\text{-}6)$$

3.3.1 Conduction and Convection Heat Transfer in the Model

In this section we outline the derivation of conduction matrix [K] and heat capacity matrix [B] introduced in Eq.(3-1) utilized by MSC/NASTRAN for modeling of heat transfer by conduction and convection.

First, consider the system with no radiation. As shown in calculus of variations the solution of heat balance Eq.(3-2) is equivalent to the minimization of the following functional:

$$I = \frac{1}{2} \iiint_V [k_x (\frac{\partial T}{\partial x})^2 + k_y (\frac{\partial T}{\partial y})^2 + k_z (\frac{\partial T}{\partial z})^2 + 2\rho C \frac{\partial T}{\partial t} T] dV$$
$$+ \frac{1}{2} \iint_S h(T - 300)^2 dS$$

(3-7)

The functional given by Eq.(3-7) is subject to boundary condition of Eq.(3-3) and initial condition of Eq.(3-6). The second integral in Eq. (3-7) includes the boundary condition of Eq.(3-4) in the value of the functional.

For each element e with P nodes we want to find temperature in its nodes T_i such that:

$$\frac{\partial I}{\partial T_i} = k \iiint_{V^{(e)}} [\frac{\partial T^{(e)}}{\partial x} \cdot \frac{\partial}{\partial T_i}(\frac{\partial T^{(e)}}{\partial x}) + \frac{\partial T^{(e)}}{\partial y} \cdot \frac{\partial}{\partial T_i}(\frac{\partial T^{(e)}}{\partial y}) +$$
$$+ \frac{\partial T^{(e)}}{\partial z} \cdot \frac{\partial}{\partial T_i}(\frac{\partial T^{(e)}}{\partial z}) + 2\rho C \frac{\partial T^{(e)}}{\partial t} \frac{\partial T^{(e)}}{\partial T_i}] dV$$

(3-8)

$$+ \iint_{S^{(e)}} h(T^{(e)} - 300) \frac{\partial T^{(e)}}{\partial T_i} dS = 0$$

Surface integral in Eq. (3-8) describes the grid points **i** that positioned on the convective boundary.

Based on Eq. (2-24) it can be shown that:

$$([K1]^{(e)} + [K2]^{(e)})T^{(e)} + [K3]\dot{T} - P^{(e)} = 0 \tag{3-9}$$

where

$$K1_{ij}^{(e)} = k\iiint\limits_{V^{(e)}}\left[\frac{\partial N_i}{\partial x}\frac{\partial N_j}{\partial x} + \frac{\partial N_i}{\partial y}\frac{\partial N_j}{\partial y} + \frac{\partial N_i}{\partial z}\frac{\partial N_j}{\partial z}\right]dV^{(e)} \tag{3-10}$$

$$K2_{ij}^{(e)} = \iint\limits_{S_{quartz}^{(e)}} hN_iN_j dS_{quartz} \tag{3-11}$$

$$K3_{ij}^{(e)} = \iiint\limits_{V^{(e)}} \rho CN_iN_j dV \tag{3-12}$$

$$P_i^{(e)} = \iint\limits_{S^{(e)}} 300hN_i dS \tag{3-13}$$

Before using the assemblage procedure, we assume that total number of grid points (nodes) in the system is M and total number of elements in the system is E. Let us define the vector T_g as the Mx1 vector of temperatures in grid points. Element characteristic matrices $[K]^{(e)}$, $[K3]^{(e)}$ and $P^{(e)}$ can be expanded to the order MxM and Mx1

respectively by adding zero terms in remaining positions. Then the characteristic matrices for the whole system are obtained as:

$$[K] = \sum_{e=1}^{E} \overline{K}^{(e)} \tag{3-14}$$

$$[B] = \sum_{e=1}^{E} \overline{K}3^{(e)} \tag{3-15}$$

$$\{P\} = \sum_{e=1}^{E} \overline{P}^{(e)} \tag{3-16}$$

where

$$[K]^{(e)} = [K1]^{(e)} + [K2]^{(e)} \tag{3-17}$$

and $\overline{K}^{(e)}$, $\overline{K}3^{(e)}$ and $\overline{P}^{(e)}$ are expanded matrices.

After substitution Eqs. (3-10) - (3-17) into Eq. (3-9), we have obtained the general equation utilized by MSC/NASTRAN for conduction and convection heat transfer:

$$[K]T_g + [B]\dot{T}_g = \{P\} \tag{3-18}$$

3.3.2 Radiation

The presence of radiation heat exchange within the system adds the nonlinear term $\{N\}$ into Eq. (3-22).The modeling of radiation exchange

between surfaces as well as other boundary heat exchange is provided through heat boundary, HBDY, elements. The HBDY elements define the heat fluxes in and out of solid elements. In finite element model of RTP system the wafer has 132 boundary elements on the top surface and 132 on the bottom surface, the chamber has 30 boundary elements, facing inside the chamber; the quartz window has 10 boundary elements on the top surface, and 10 on the bottom surface, each lamp is described by one boundary element, faced the rest of the model.

3.3.2.1 View Factors and Radiation Exchange Coefficients

During the first run NASTRAN activates VIEW module. The VIEW module utilizes HBDY geometry information to calculate the view factors between surfaces taking into account any shading caused by the other surfaces.

There exists a non-zero view factor between element 1 and 2 if the following two conditions are satisfied simultaneously [5]:

$$\cos \alpha > 0, \cos \beta > 0 \qquad (3\text{-}19)$$

where α and β are angles between the vector connecting centroids of elements 1 and 2 and the vectors normal to element 1 and 2 respectively as shown in Figure 7.
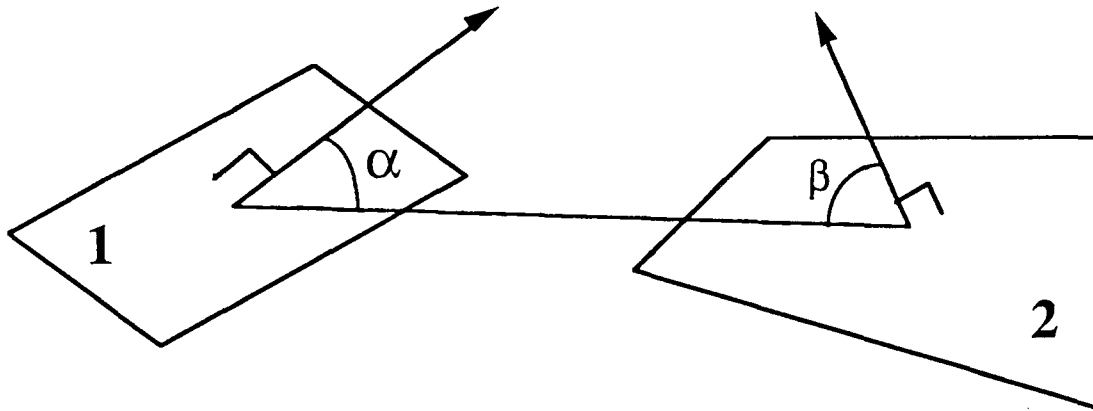
Figure 7 Non-zero view factor angles

In case of shading by external surfaces or mutual positioning of elements for which conditions (3-19) are not satisfied, the accuracy of calculated view factors may be very poor. The VIEW module allows to define a subelements mesh for any element in order to improve the results of calculation. The view factors will be calculated between all subelements and then combined to produce a view factor for elements which they comprise. The accuracy of view factors directly depends on what mesh is used. The mesh used for wafer consists of 2x2 subelements for bottom surface and 3x3 for top surface, the same as for lamps. The mesh used for quartz window consists of 10 subelements along the radius by 2 subelements of the sectors. The mesh for chamber walls consists of 15 subelements along the height by 3 subelements along the circumvence. The mesh for bottom of the chamber consists of 1x2 is subelements.

Several analytic procedures have been developed for evaluation of Eq. (2-10). Contour integral and finite difference methods are available in the

VIEW module. The finite difference method requires less computer time but becomes inaccurate when $A_i/r^2_{ij} > 0.1$,where A_i is a subelement area and r_{ij} is a distance between subelements. The contour integral method is more expensive but produces more accurate results. The user may select the method of computation or leave the choice to MSC/NASTRAN, which will use contour integral method only if $A_i/r^2_{ij} > RMAX$. The value of RMAX may be specified by user. Due to complexity of considered RTP process model several computational experiments was conducted and the second alternative with RMAX=0.1 has been selected as the best trade off.

The output from the first run is the symmetric view factor matrix F computed based on Eqs (2-9) and (2-10) punched into RADMXT cards. This matrix completely describes the geometry of the model and MSC/NASTRAN will use it for calculation of heat exchange between the radiative surfaces.

MSC/NASTRAN assumes the radiative elements to be gray, diffuse and opaque. Then for any closed model

$$Aq^{in} = Fq^{out} \qquad (3\text{-}20)$$

where A is diagonal matrix of elements areas, F - view factor matrix, q^{in} - vector of incoming thermal radiation heat into elements, q^{out} - vector of outcoming radiation from elements.

The outcoming radiation per unit area is given by:

$$q^{out} = \sigma E_\varepsilon \, T_e^4 + (I - E_\alpha)q^{in} \qquad (3\text{-}21)$$

where

E_ε, E_α – are the diagonal matrices of emissivities and absorptivities respectively,

σ – is the Stefan - Boltzmann constant,

T_e - is the temperature vector ,

I - identity matrix.

Substitution of Eq (3-21) into Eq (3-20) gives

$$q^{in} = \sigma(A - F(I - E_\alpha))^{-1} F E_\varepsilon T_e^4 \qquad (3\text{-}22)$$

The radiative heat flow into finite element is given as

$$Q_e = (q^{in} - q^{out})A \qquad (3\text{-}23)$$

After the substitution of Eqs (3-21) and (3-22) in Eq.(3-23) we obtain:

$$Q_e = -\sigma[AE_\varepsilon - AE_\alpha[A - F(I - E_\alpha)^{-1} F E_\varepsilon]]T_e^4 = R_e T_e^4 \quad (3\text{-}24)$$

where R_e is called element radiation heat flow exchange matrix.

The transformation from element heat flow to grid points heat flow is given by:

$$Q_g = G^T Q_e \qquad (3\text{-}25)$$

where

G - is matrix formed from vectors of fractions of total area of finite element attributed to each grid of its points.

The interpolation of the temperature in the grid point is given by:

$$T_e^4 = GT_g^4 \qquad (3\text{-}26)$$

Substitution of Eqs.(3-29) and (3-30) gives the formula describing the radiation heat rate relations between the grid points in the model:

$$Q_g = -G^T R_e GT_g^4 = -[R_{gg}]T_g^4 \qquad (3\text{-}27)$$

where

$R_{gg} = G^T \sigma[AE_\varepsilon - AE_\alpha[A - F(I - E_\alpha)^{-1} FE_\varepsilon]]G$ is the matrix of radiation exchange between the grid points of the model. The R_{gg} matrix is calculated by RMG module [10] and then used directly in conjunction with other data to calculate the temperature distribution.

3.3.2.2 Modeling of Semitransparent Quartz Window

Most of the commercially available finite element software packages (NASTRAN, ANSYS, PATRAN, etc.) were initially developed for structural analysis and have limited capabilities in terms of heat transfer analysis. Thus, MSC/NASTRAN package does not have the capability of analyzing radiation heat exchange for systems with semitransparent components. In particular, the generation of the view factors is performed based on the assumption that all elements are opaque.

Therefore, to correctly model the transmission of the radiation through quartz window at the top of the RTP chamber the view factors generated by VIEW module should be recalculated to allow for radiation exchange between halogen lamps and the silicon wafer in the presence of partial shading by quartz window.

Selected in this thesis approach to the modeling of the radiation exchange through semitransparent window is based on the substitution of the general model of RTP system with the "equivalent" model consisting of only opaque bodies. In order to illustrate this concept let us consider the simplified model of the system consisting of radiative source (lamps), opaque body (silicon wafer and chamber) and semitransparent body (quartz window) between them as shown in the Figure 8.
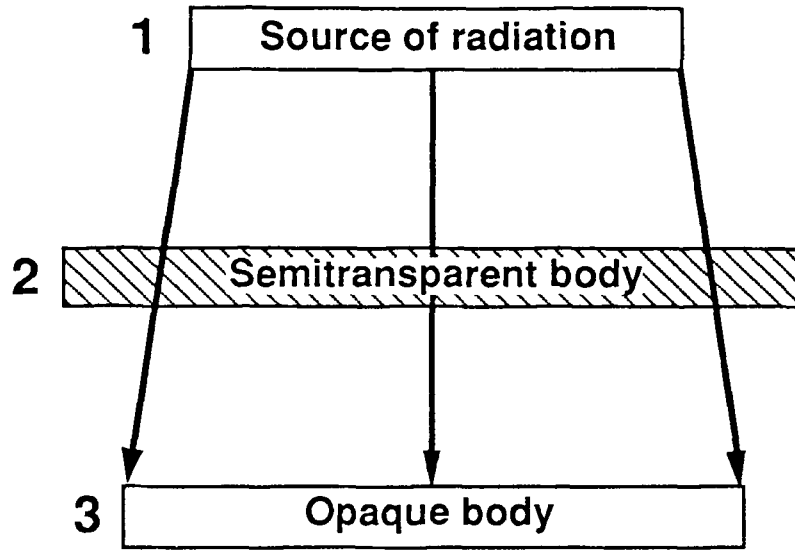
Figure 8. Simplified model of RTP system.

Utilizing the relationship given by Eqs. (3-21) and (3-22) the radiation exchange within the above system can be described by

$$q_1^{out} = \sigma E_\varepsilon^{(1)} T_1^4 + (I - E_\alpha^{(1)}) q_1^{in} \tag{3-28}$$

$$A_1 q_1^{in} = F_{1 \to 1} q_1^{out} + F_{2 \to 1} q_2^{out} + F_{3 \to 1} E_\tau^{(2)} q_3^{out} \tag{3-29}$$

$$q_2^{out} = \sigma E_\varepsilon^{(2)} T_2^4 + (I - E_\alpha^{(2)} - E_\tau^{(2)}) q_2^{in} \tag{3-30}$$

$$A_2 q_2^{in} = F_{1 \to 2} q_1^{out} + F_{2 \to 2} q_2^{out} + F_{3 \to 2} q_3^{out} \tag{3-31}$$

$$q_3^{out} = \sigma E_\varepsilon^{(3)} T_3^4 + (I - E_\alpha^{(3)}) q_3^{in} \tag{3-32}$$

$$A_3 q_3^{in} = F_{1 \to 3} E_\tau^{(2)} q_1^{out} + F_{2 \to 3} q_2^{out} + F_{3 \to 3} q_3^{out} \qquad (3\text{-}33)$$

where E_τ is the diagonal matrix of transmittance, $F_{i \to j}$ are symmetric matrices of view factors computed by VIEW module under the assumption that quartz window is 100% transparent.

The equivalent model of RTP system should consist of only opaque elements and preserve the net heat balance for each component of the system. In other words the difference between absorbed and emitted radiation by each element should remain the same as in original model. These requirements can be expressed as:

$$E_\alpha^{(i),new} q_{i,new}^{in} - \sigma E_\varepsilon^{(i),new} T_i^4 = E_\alpha^{(i)} q_i^{in} - \sigma E_\varepsilon^{(i)} T_i^4 \qquad (3\text{-}34)$$

where subscript "new" denotes the parameters of the new model consisting of only opaque elements.

The presence of the semitransparent quartz window has the effect of the reduction in direct illumination of RTP chamber and wafer by the halogen lamps radiation and can be modeled by the following adjustment of view factor matrix:

$$F_{1 \to 3}^{new} = E_\tau F_{1 \to 3} = E_\tau F_{3 \to 1} = F_{3 \to 1}^{new} \qquad (3\text{-}35)$$

In order to keep the differences between "original" and "equivalent" model to the minimum we would like to preserve the following values:

$$E_\alpha^{(1),new} = E_\alpha^{(1)}; \quad E_\varepsilon^{(1),new} = E_\varepsilon^{(1)}$$

$$E_\alpha^{(3),new} = E_\alpha^{(3)}; \quad E_\varepsilon^{(3),new} = E_\varepsilon^{(3)} \qquad (3\text{-}36)$$

$$F_{1-1}^{new} = F_{1-1}; \quad F_{3-3}^{new} = F_{3-3}$$

Taking into account Eqs. (3-34) - (3-36) and assuming the quartz transmission in new model, E_τ^{new}, equal to zero the radiation exchange within the model can be described as

$$q_1^{out,new} = \sigma E_\varepsilon^{(1),new} T_1^4 + (I - E_\alpha^{(1),new}) q_1^{in,new} \qquad (3\text{-}37)$$

$$A_1 q_1^{in,new} = F_{1-1}^{new} q_1^{out,new} + F_{2-1}^{new} q_2^{out} + F_{3-1}^{new} q_3^{out,new} \qquad (3\text{-}38)$$

$$q_2^{out,new} = \sigma E_\varepsilon^{(2),new} T_2^4 + (I - E_\alpha^{(2),new}) q_2^{in,new} \qquad (3\text{-}39)$$

$$A_2 q_2^{in,new} = F_{1-2}^{new} q_1^{out,new} + F_{2-2}^{new} q_2^{out,new} + F_{3-2}^{new} q_3^{out,new} \qquad (3\text{-}40)$$

$$q_3^{out,new} = \sigma E_\varepsilon^{(3),new} T_3^4 + (I - E_\alpha^{(3),new}) q_3^{in,new} \qquad (3\text{-}41)$$

$$A_3 q_3^{in,new} = F_{1-3}^{new} q_1^{out,new} + F_{2-3}^{new} q_2^{out,new} + F_{3-3}^{new} q_3^{out,new} \qquad (3\text{-}42)$$

The system consisting of Eqs (3-28) - (3-42) can now be solved for unknown values of $E_\alpha^{(2),new}$, $E_\varepsilon^{(2),new}$, $F_{2-1}^{new} = F_{1-2}^{new}, F_{2-2}^{new}, F_{2-3}^{new} = F_{3-2}^{new}$.

Assuming that the values of emissivities and absorptivities are scalars within each component of the model, the solution can be expressed as:

$$E_\varepsilon^{(2),new} = E_\varepsilon^{(2)} \frac{1-E_\tau^{(2)}}{1-E_\tau^{(2)}-E_\tau^{(2)}E_\alpha^{(2)}} \qquad (3\text{-}43)$$

$$E_\alpha^{(2),new} = E_\alpha^{(2)} \frac{1-E_\tau^{(2)}}{1-E_\tau^{(2)}-E_\tau^{(2)}E_\alpha^{(2)}} \qquad (3\text{-}44)$$

$$F_{2-1}^{new} = F_{1-2}^{new} = (1-E_\tau)F_{1-2} \qquad (3\text{-}45)$$

$$F_{2-2}^{new} = (1-E_\tau)^2 F_{2-2} + E_\tau A_2 \qquad (3\text{-}46)$$

$$F_{2-3}^{new} = F_{3-2}^{new} = (1-E_\tau)F_{3-2} \qquad (3\text{-}47)$$

The new model of the radiation exchange within the RTP system given by Eqs (3-35) - (3-47) is equivalent to the original model of RTP system given by Eqs (3-28) - (3-33) in terms of preservation of net heat exchange between model elements. On the other hand the new model does not contain any semitransparent elements not supported by MSC/NASTRAN.

The new view factor matrix F^{new} can now be represented as:

$$F^{new} = \begin{bmatrix} F_{1-1} & F_{1-2}^{new} & F_{1-3}^{new} \\ F_{2-1}^{new} & F_{2-2}^{new} & F_{2-3}^{new} \\ F_{3-1}^{new} & F_{3-2}^{new} & F_{3-3} \end{bmatrix}$$

In order to obtain the components of matrix F^{new} the special purpose program was developed. This program takes its input from the output of MSC/NASTRAN VIEW module, modifies the values of view factors according to Eqs (3-49) - (3-51) and (3-39) and outputs the modified view factor matrix according to the format of MSC/NASTRAN RADMTX Bulk Data cards. The RADMTX cards allow to specify the view factor matrix directly by passing the execution of VIEW module. The modified view factor matrix F^{new} entered through the set of RADMTX cards can now be used for computation of radiation exchange matrix R_{gg} given in Eq (3-27).The listing of the program used for generation of RADMTX cards is given in Appendix.

CHAPTER 4

RADIATION EXCHANGE COEFFICIENTS FOR REAL TIME CONTROL ALGORITHM

In this chapter we will describe the computation of generalized radiation exchange coefficients based on view factor data generated by the finite element model of RTP system. This information allows for accurate description of the RTP system in real-time control software developed at NJIT Electronic Imaging Center by Dr. Belikov.

4.1 Generalized Model of RTP System

The generalized model of RTP system used for realization of real time control algorithm is built based on the fact that the number of points in which the temperature of wafer can be measured is limited. This fact dictates that the number of elements in the model should be equal to the number of such points. The generalized model of RTP system does not explicitly describe the geometry of RTP chamber. Instead, the effective radiation exchange between the source of radiation (halogen lamps) and object of interest (silicon wafer) is considered in the model. Within the generalized model the structure of RTP system is assumed to be axisymmetric. The halogen lamps are approximated as three concentric lamp zones and the wafer is modeled as a collection of concentric elements.

The differences between finite element and generalized models are illustrated in Figure 9.
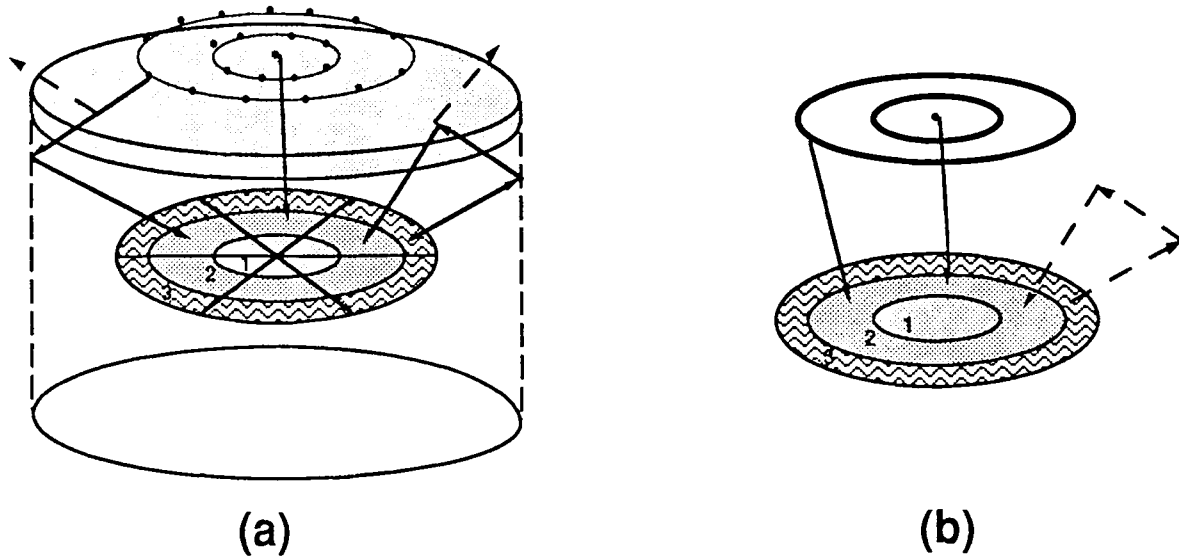

(a)   **(b)**

Figure 9 Schematics of RTP system models: (a) Finite Element model - calculation of radiation exchange coefficients takes into account internal reflections, absorption and transmittance; (b) Model utilized in real-time control algorithm - generalized radiation exchange coefficients are based on the data computed via finite element model.

Based on these assumptions, the radiation absorbed by i-th concentric element of the wafer can be described as [11]:

$$q_i^{abs} = \sum_{j=1}^{J} L_{i,j} P_j + \sum_{k=1}^{K} W_{i,k} q_k^{em} \qquad (4\text{-}1)$$

where

q_k^{em} - is the radiation emitted by K-th zone of the wafer,

$L_{i,j}, W_{i,k}$ - are the fractions of the power radiated by lamp zone j and by the wafer element k respectively that are absorbed by the i-th zone of the wafer

P_j- is the power radiated by lamp zone j

The coefficient $W_{i,k}$ is given by

$$W_{i,k} = \frac{\varepsilon_k^t}{\varepsilon_k^t + \varepsilon_k^b}(G_{i,k}^{t-t} + G_{i,k}^{b-t}) + \frac{\varepsilon_k^b}{\varepsilon_k^t + \varepsilon_k^b}(G_{i,k}^{t-b} + G_{i,k}^{b-b}) \qquad (4\text{-}3)$$

where:

ε_k^t and ε_k^b -   are the emissivities of the top and bottom surfaces of k-th wafer element respectively,

$G_{i,k}^{b-t}$ and $G_{i,k}^{b-b}$ -   are the fractions of radiation emitted by the bottom surface of i-th wafer zone that is absorbed by the top and bottom of k-th wafer element respectively,

$G_{i,k}^{t-t}$ and $G_{i,k}^{t-b}$ -   are the fractions of radiation emitted by the top surface of i-th wafer zone that is absorbed by the top and bottom of k-th wafer element respectively.

In the case of equal emissivities of top and bottom surfaces of the wafer the generalized coefficients $W_{i,k}$ can be represented as

$$W_{i,k} = \frac{1}{2}(G_{i,k}^{t-t} + G_{i,k}^{b-t}) + \frac{1}{2}(G_{i,k}^{t-b} + G_{i,k}^{b-b}) \qquad (4\text{-}3)$$

The coefficient $L_{i,j}$ introduced in Equation (4-1) is given by

$$L_{i,j} = G_{i,j}^{l-t} + G_{i,j}^{l-b} \qquad (4-4)$$

where $G_{i,j}^{l-t}$ and $G_{i,j}^{l-b}$ - are the fractions of radiation emitted by the j-th lamp zone that are absorbed by top and bottom surfaces of the i-th wafer zone respectively.

4.2 Computation of Generalized Radiation Exchange Coefficients

In order to correctly compute the matrices of generalized radiation exchange coefficients W and L introduced in Eq. (4-1) the radiation exchange between all components of RTP system has to be taken into account. These computations are based on the detailed finite element model of RTP system described in the previous chapter. Utilization of the finite element model allows for accurate computation of the geometry and radiative properties of the entire RTP system. This approach provides real time control software with realistic values of effective fluxes of radiation and relieves the real time software from computationally expensive analysis of radiation exchange within complex geometry of RTP system.

4.2.1 Radiation Exchange Matrix

The first step in computation of matrices W and L involves the consideration of radiation exchange between all elements of detailed finite element model of RTP system, which can be expressed as:

$$q^{abs} = \tilde{R}q^{em}, \qquad (4\text{-}5)$$

where

q^{abs} - is the vector of radiation absorbed by the elements of the RTP model,

q^{em} - is the vector of radiation emitted by all elements of the RTP model,

$\tilde{R}$ - is the matrix of radiation exchange coefficients r_{ik}, where r_{ik} represents the fraction of radiation emitted by the i-th element of the model that is absorbed by the k-th element.

The actual computation of the elements of the generalized radiation exchange matrix G takes into account the reflection, absorption and transmittance of radiation within entire RTP system as given by Eqs. (4-5) - (4-7). Thus, the radiation absorbed by the elements of the model, q^{abs}, can be expressed as:

$$q^{abs} = E_{\alpha}q^{in} = E_{\alpha}\sigma(A - F(I - E_{\alpha}))^{-1}FE_{\varepsilon}T^{4} \qquad (4\text{-}6)$$

where F - is the matrix of view factors calculated taking into account the transmittance of quartz window.

On the other hand, the radiation emitted by the elements of the model, q^{em}, can be expressed based on the Stefan-Boltzmann law as:

$$q^{em} = \sigma E_\varepsilon T^4 \tag{4-7}$$

After substitution of Eq. (4-7) into Eq. (4-6) we obtain

$$q^{abs} = E_\alpha (A - F(I - E_\alpha))^{-1} F q^{em} \tag{4-8}$$

and, therefore, the radiation exchange matrix $\tilde{R}$ is given by:

$$\tilde{R} = E_\alpha (A - F(I - E_\alpha))^{-1} F. \tag{4-9}$$

4.2.2 Radiation Exchange Between Zones of Generalized Model

The calculation of radiation exchange coefficients between wafer and lamp zones utilized in real time control algorithm is based on the fact that each zone in generalized model can be considered as a collection of particular finite elements. Real time control algorithm models the lamp zones of the RTP system by three rings of lamps and subdivides the wafer into M annular wafer zones.

We will define a subzone of the wafer as a collection of identical finite elements positioned at the same distance from the center of the wafer. In our finite element model there are 11 subzones on the wafer. Then each of

M zones is considered as a collection of subzones, where the number of subzones in each zone is $n_1,...,n_m$.

Let us consider radiation exchange between one lamp zone l consisting of L_1 lamps and all wafer subzones. Total radiation emitted from lamp zone l that is absorbed by the i-th finite element of the wafer is:

$$Q_{lamp\ zone\ l,i} = \sum_{j \in l} q_j^{em} r_{ji} \qquad (4\text{-}10)$$

Or in the case of lamp zones consisting of identical lamps:

$$Q_{lamp\ zone\ l,i} = q_{L_1}^{em} \sum_{j \in l} r_{ji} \qquad (4\text{-}11)$$

Therefore, fraction of radiation emitted by lamp zone l that is absorbed by the i-th wafer element is given by:

$$\frac{Q_{lamp\ zone\ l,i}}{Q_{lamp\ zone\ l\ total}} = \frac{q_{L_1}^{em} \sum_{j \in l} r_{ji}}{L_1 q_{L_1}^{em}} = \frac{1}{L_1} \sum_{j \in l} r_{ji} \qquad (4\text{-}12)$$

The total radiation emitted by lamp zone l that is absorbed by the k-th wafer subzone is given by:

$$Q_{lamp\ zone\ l,wafer\ subzone\ k} = \sum_{i \in k} Q_{lamp\ zone\ l,i} \qquad (4\text{-}13)$$

Then the radiation exchange coefficients for subzones $S_{i,k}^{l-t}$ and $S_{i,k}^{l-b}$ representing the fraction of radiation emitted by lamp zone l that is absorbed by the top and bottom of the wafer subzone k given by:

$$S_{l,k}^{l-t} = \frac{Q_{\text{lamp zone l,wafer subzone k}}^{\text{top}}}{Q_{\text{lamp zone l total}}} = \frac{\sum_{i\in k} Q_{\text{lamp zone l,i}}}{L_l q_{L_l}^{em}} = \frac{\sum_{i\in k^{\text{top}}} \sum_{j\in l} r_{ji}}{L_l} \quad (4\text{-}14)$$

$$S_{l,k}^{l-b} = \frac{Q_{\text{lamp zone l,wafer subzone k}}^{\text{bottom}}}{Q_{\text{lamp zone l total}}} = \frac{\sum_{i\in k^b} \sum_{j\in l} r_{j,i}}{L_l} \quad (4\text{-}15)$$

Applying the same consideration to computation of radiation exchange coefficients between wafer subzones i and k the matrices $S_{i,k}^{t/b-t/b}$ are found to be:

$$S_{i,k}^{t/b-t/b} = \frac{\sum_{n\in k^{t/b}} \sum_{j\in i^{t/b}} r_{jn}}{N} \quad (4\text{-}16)$$

where N - is the number of finite elements in a wafer zone.

We now consider the m-th wafer zone consisting of n_m wafer subzones. The radiation exchange between lamp zone l and wafer zone n is given by:

$$G_{l,m}^{l-t} = \sum_{k^{\text{top}}\in m} S_{l,k}^{l-t} = \sum_{k^{\text{top}}\in m} \frac{\sum_{i\in k^{\text{top}}} \sum_{j\in l} r_{j,i}}{L_l} \quad (4\text{-}17)$$

The radiation exchange coefficients between wafer zones themselves cannot be obtained from the previous consideration because the subzones within a wafer zone are not identical.

The radiation from wafer zone m that is absorbed by wafer subzone k is

$$Q_{\text{wafer zone m,wafer subzone k}} = \sum_{j \in l} q_j^{em} S_{jk} \qquad (4\text{-}18)$$

where $q_j^{em} = \sigma A_j E_\varepsilon^{(j)} T_j^4$ is radiation emitted by the j-th subzone inside the wafer zone m.

The RTP model for real time control algorithm assumes that the temperatures and emissivities within any wafer zone do not change, therefore the ratio of radiation absorbed by wafer subzone k to radiation emitted by wafer zone m is:

$$\frac{Q_{\text{wafer zone m,wafer subzone k}}}{Q_{\text{wafer zone m total}}} = \frac{\sum\limits_{i \in m} A_i S_{ik}}{\sum\limits_{i \in m} A_i} \qquad (4\text{-}19)$$

Therefore, the radiation exchange coefficient between wafer zones m and n is given by:

$$G_{mn} = \sum_{k \in n} \frac{Q_{\text{wafer zone m,wafer subzone k}}}{Q_{\text{wafer zone m total}}} = \sum_{k \in n} \frac{\sum\limits_{i \in m} A_i S_{ik}}{A_m} \qquad (4\text{-}20)$$

where A_i is an area of the i-th wafer subzone and A_m is an area of the m-th wafer zone.

In order to obtain the generalized radiation exchange coefficients given by Eq. (4-17) and Eq. (4-20) the new solution sequence utilizing DMAP (Direct Matrix Abstraction Programming) language has been developed. This solution sequence allows to specify each of the wafer zones and then computes radiation exchange coefficients between lamp and wafer zones and between wafer zones. The listing of the solution sequence can be found in the Appendix.

CHAPTER 5
APPLICATION OF FEM TO THERMAL ANALYSIS OF RTP SYSTEM

In this chapter we will consider the calibration of the finite element model of RTP system based on the available experimental data. Utilizing the calibrated model we will analyze the temperature profile on the silicon wafer as function of the temperatures of tungsten-halogen lamps. We will also consider the requirements for the uniform heating of silicon wafer according to prescribed temperature trajectory. Finally, we will analyze the disturbance of the wafer temperature profile caused by the presence of K-type thermocouple attached to the wafer surface.

5.1 Calibration of Finite Element Model

The finite element model described in Chapter 3 is based on a number of simplifying assumptions:

1. Emittance is assumed to be gray and diffusive;

2. Thermal conductivity is assumed to be isotropic and temperature-independent;

3. Only the major components of RTP system are modeled. The effects of such components as wafer holder, gas shower, and ambient atmosphere do not directly enter the model.

Due to the above assumptions as well as the lack of the accurate information about the thermal and radiometric characteristics of the components of RTP system, there is a need for evaluation of the effective values of system parameters in order to utilize the finite element model for analysis of thermal behavior of actual system.

In order to estimate the effective values of thermal and radiometric parameters the simplified model of RTP system was developed to approximate the behavior of the finite element model. This simplified model assumes the one-dimensional (radial) variation of wafer temperature and utilizes the finite difference approach to imitate the behavior of finite element model. The simplified model approximates the temperature gradient in 11 points along the radius of the wafer corresponding to the 11 radial elements of the finite element model according to the following heat balance equation:

$$C_v V_i \frac{\partial T_i}{\partial t} = \sum_{m=1}^{3} q_m^{em,lamp} \cdot g_{m,i}^{lamp} + \sum_{n=1}^{3} q_n^{em,wafer} \cdot g_{n,i}^{wafer} - \varepsilon\sigma A_i T_i^4 -$$
$$-kA_{i-1,i} \frac{T_i - T_{i-1}}{r_i - r_{i-1}} - kA_{i,i+1} \frac{T_i - T_{i+1}}{r_{i+1} - r_i} \qquad (5\text{-}1)$$

where:

T_i - is the temperature of the i-th radial point,

A_i - is the surface area of the finite element corresponding to the i-th radial point,

$A_{i,j}$ - is the crossectional area between the i-th and j-th element,

r_i - is the radial coordinate of the i-th radial point,

V_i - is the volume of the finite element corresponding to the i-th radial point,

$q_n^{em,wafer}$, $q_m^{em,lamp}$ - are the radiation fluxes emitted by the m-th ring of lamps and the n-th ring of wafer elements respectively,

$g_{n,i}^{wafer}$, $g_{m,i}^{lamp}$ - are the radiation exchange coefficients between the i-th wafer element and the n-th ring of wafer elements and m-th zone of lamps respectively.

In the model specified by the system of equations (5-1) the temperatures in the 11 points along the wafer radius can be considered as functions of several variables:

$$T_i = f(t,k,\varepsilon,T^{lamp-zones}) \qquad (5-2)$$

where thermal conductivity k, emissivity ε, and the temperatures of the lamp zones $T^{lamp-zones}$, are the design parameters. Our objective is to find the values of this parameters such that the deviation between the simulated temperatures $T(t,k,\varepsilon,T^{lamp-zones})$ and experimentally measured temperatures $T^{exp}(t)$ is minimized within a given interval of time Δt.

In the case of experimental measurements of the wafer temperature with the four thermocouples the vectors of experimentally measured and simulated temperatures can be represented as:

$$T^{exp}(t) = \begin{Bmatrix} T_1(t) \\ .... \\ T_4(t) \end{Bmatrix} \quad \text{and} \quad T(t,k,\epsilon,T^{lamp-zones}) = \begin{Bmatrix} T_1(t,k,\epsilon,T^{lamp-zones}) \\ .... \\ T_4(t,k,\epsilon,T^{lamp-zones}) \end{Bmatrix}.$$

The deviation between the experimentally measured and simulated temperatures at any moment of time, $E(t) = T^{exp}(t) - T(t,k,\epsilon,T^{lamp-zones})$ is 4x1 vector with the length given by Euclidean norm:

$$|E(t)| = \sqrt{\sum_{j=1}^{4} E_j^2(t)} = \sqrt{\sum_{j=1}^{4} \left(T_j(t) - T(t,k,\epsilon,T^{lamp-zones})\right)^2} \qquad (5\text{-}3)$$

In order to obtain accurate estimate of system parameters the experimental data corresponding to various modes of the wafer heating should be utilized in calibration. For n-th set of the experimental measurements the largest deviation between measured and simulated values of temperatures over the time of entire experiment can be expressed as:

$$F^n = \max_{t \in \Delta t^n} \sqrt{\sum_{j=1}^{4} \left(T_j^{exp,n}(t) - T_j^n(t,k,\epsilon,T^{lamp-zones})\right)^2} \qquad (5\text{-}4)$$

In the chosen calibration algorithm we will minimize the largest deviation F^n among all available sets of experimental measurements. In our case the calibration was based on two experimental runs, first of which corresponds to the heating the wafer for 85 seconds with only central lamp turned on, and the second run corresponds to the wafer heating for 19 seconds with only outer zone of lamps turned on. In this case the problem of calibration of the finite element model of RTP system was stated as follows:

$$\min_{k,\varepsilon,T^{lamps}} \left\{\max(F^1,F^2)\right\} \to k,e,T^{lamp-zones} \qquad (5\text{-}5)$$

where:

$$
\begin{aligned}
F^1 &= \max_{t\in[0;85]} \sqrt{\sum_{j=1}^{4}\left(P_j^1(t)-T_j^1(t,k,\varepsilon,T^{central\ lamp})\right)^2} \\
F^2 &= \max_{t\in[0;19]} \sqrt{\sum_{j=1}^{4}\left(P_j^2(t)-T_j^2(t,k,\varepsilon,T^{outer\ lamp-zone})\right)^2}
\end{aligned}
\qquad (5\text{-}6)
$$

where $P_j^1(t)$ and $P_j^2(t)$ represent the polynomial approximations of data from both experimental runs.

The calibration problem given by Eq. (5-5) was solved by MATLAB software package and the effective value of wafer conductivity was found to be 1.3 Cal/inch s K, whereas the effective value of wafer emissivity was determined as 0.51.

The comparison of the experimental measurements with simulation results based on the described above effective values of the model parameters is shown in Figures 10 - 13. The transient behavior of the temperature at the central and edge points of the wafer (corresponding to the positions of thermocouples T1 and T4) for cases of wafer heating with only central lamp and with only outer zone of lamps are shown in Figures 10 and 11 respectively. The corresponding radial temperature profiles are shown in Figures. 12 and 13.
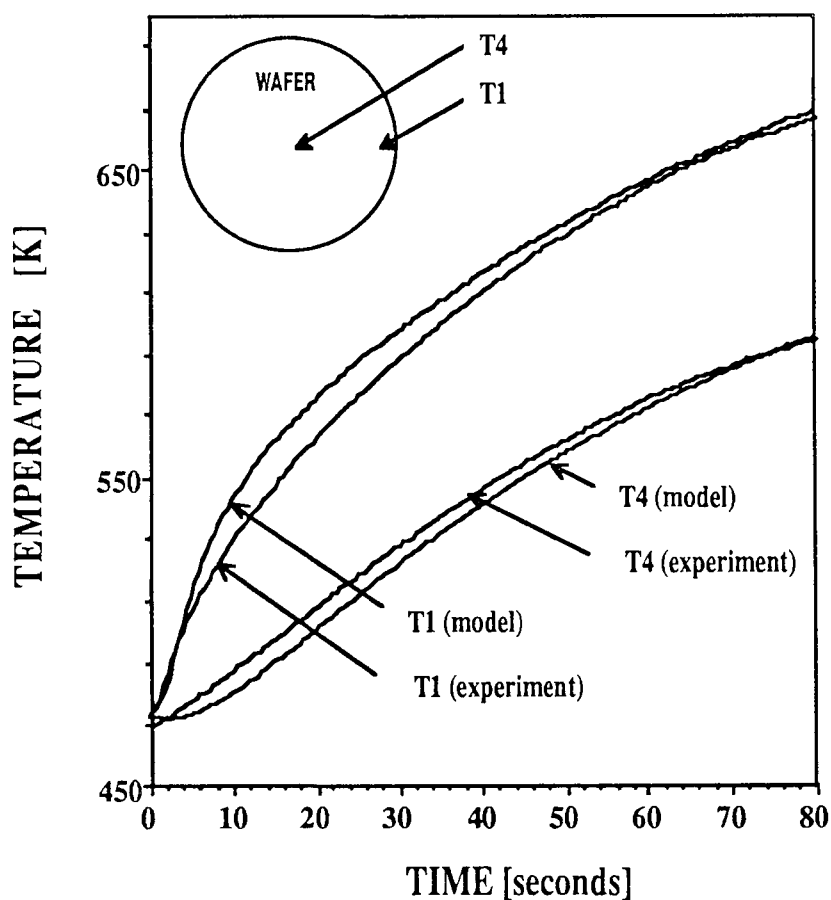

Figure 10. Temperatures of center and edge of the wafer resulting from heating by central lamp.

In the case of heating with only central lamp the simulated effective radiant power[1] of the lamp is equal to 343W. The value of simulated effective radiant power for the case of wafer heating by the outer zone of lamps is equal to 390W for each lamp. The inspection of Figure 10 shows that there is approximately 10° deviation between the simulated and experimentally obtained temperature profiles when the wafer temperature is comparatively low. This deviation can be attributed to the modeling of the temperature dependent conductivity [12] of the wafer by a constant value obtained from overall fit to experimental data.
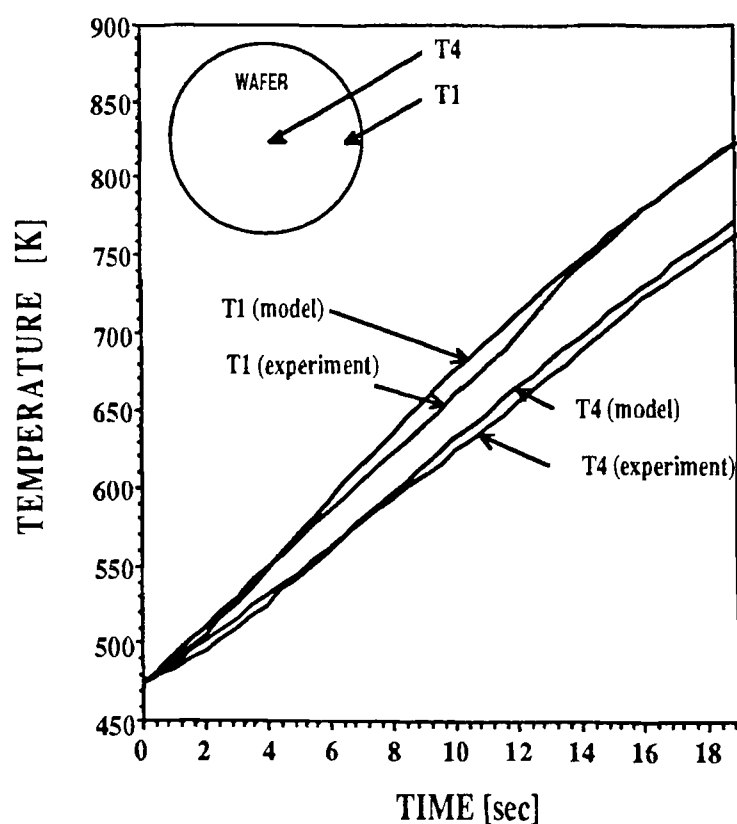

Figure 11. Temperatures of center and edge of the wafer resulting from heating by outer zone of lamps.

---

[1] Here the term "effective radiant power" means the radiant power of the lamp which would be needed to produce the temperature profile under consideration if the actual system exactly conformed to the assumtions of the model.
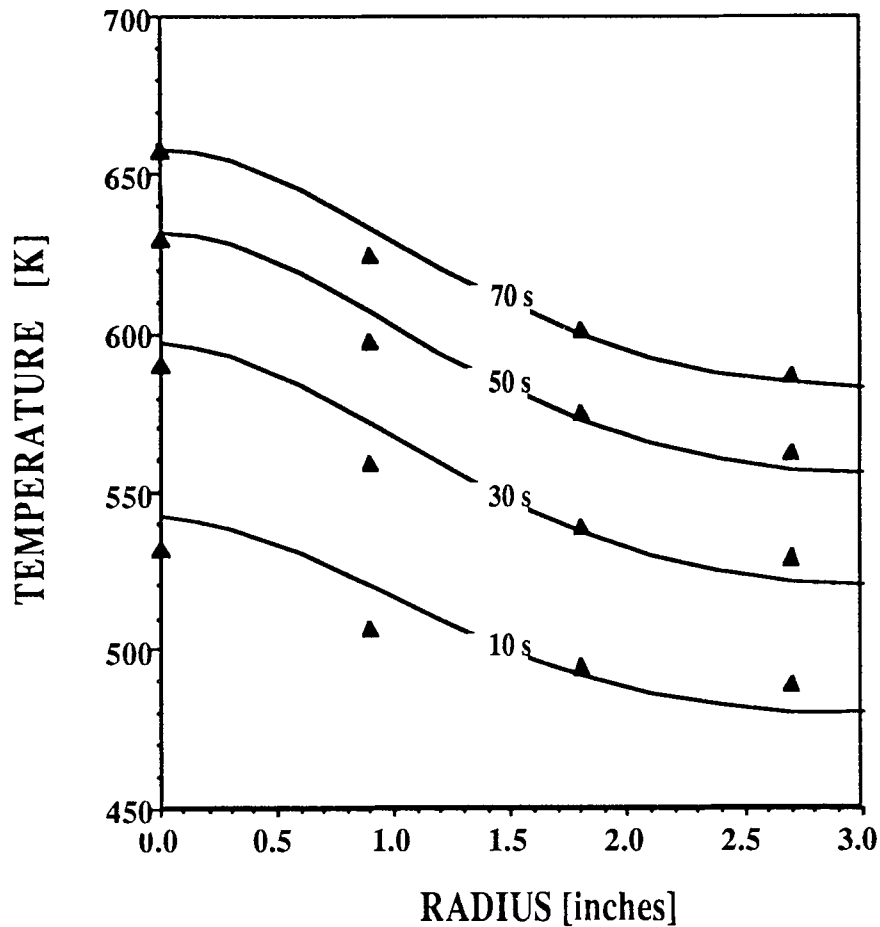
Figure 12. Radial temperature profile of the wafer resulting from heating by central lamp.

On the other hand, the inspection of Figure 11 shows comparatively better correspondence between experimentally measured and simulated transient behavior of the system. This improvement is due to the fact that in the case of wafer heating by outer zone of lamps the radiation heat exchange dominates the heat transfer by conduction since the source of radiation is less localized. In this situation the effect of temperature-dependent thermal conductivity is less pronounced.
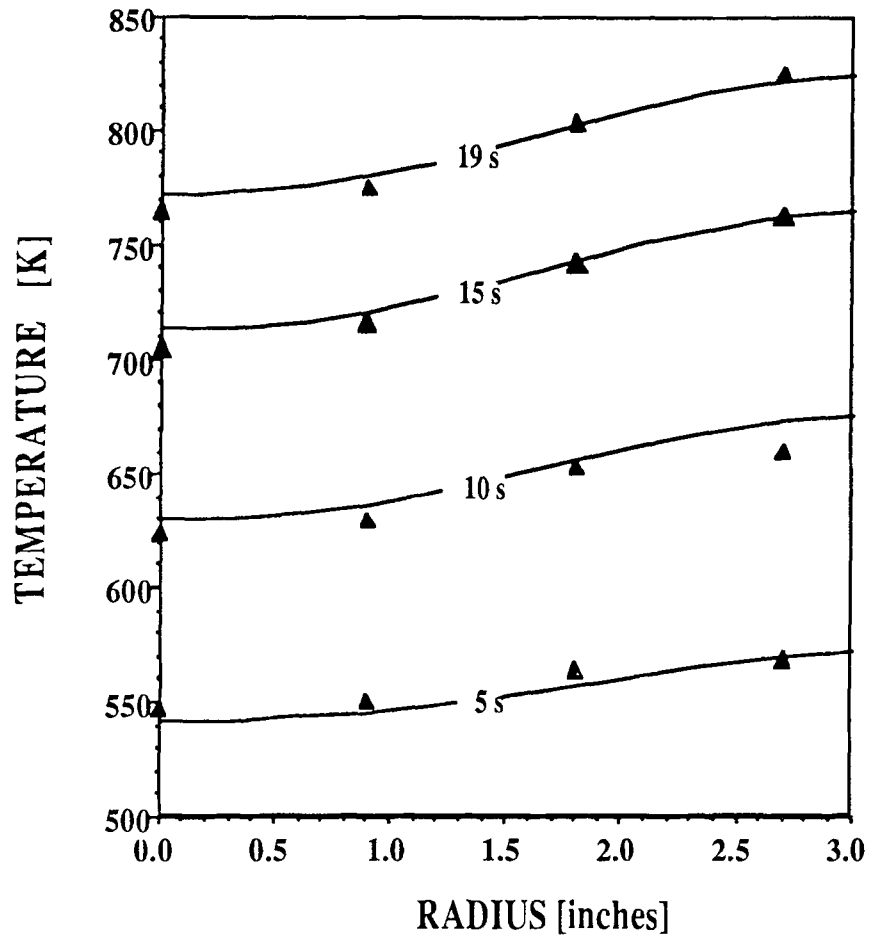
Figure 13. Radial temperature profile of the wafer resulting from heating by outer zone of lamps.

The inspection of Figures 12 and 13 show good correspondence between experimentally measured and simulated temperature profiles along the radius of the wafer.

5.2 Analysis of Simulation Results

The calibrated finite element model of RTP chamber was utilized for analysis of wafer temperature profiles for various heating conditions*. The temperature profile resulting from heating of the wafer by all lamps with effective radiant power at each lamp equal to 225W are illustrated in Figure 14. The inspection of this figure shows that the time constant in this case is about 30 seconds and that the wafer temperature profile is characterized by the lower temperatures at the edge of the wafer.

Temperature (K)

LEGEND
Time = 10s
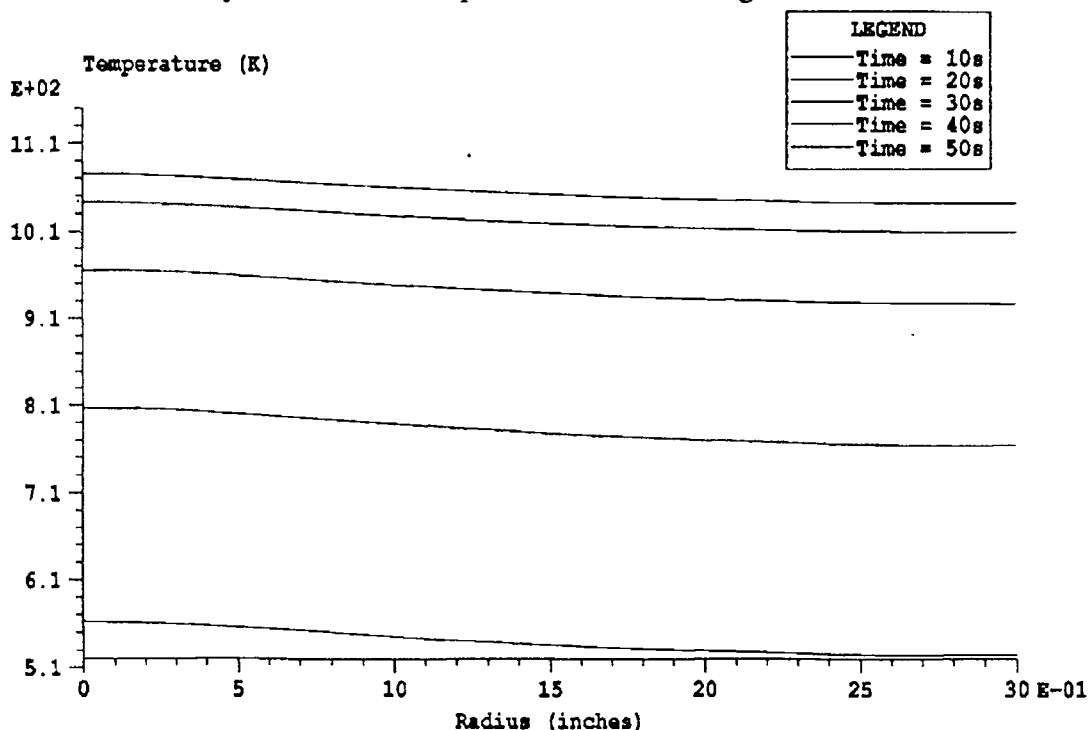Time = 20s
Time = 30s
Time = 40s
Time = 50s

Radius (inches)

Figure 14. Radial temperature profile of the wafer resulting from heating by all lamp zones with equal effective emitting power of 225W per lamp.

---

* The initial temperature of all components of the system was assumed to be 300K.

In order to analyze the effect of each lamp zone on the wafer temperature profile the wafer heating by each individual lamp zone was simulated for equal values of radiant power per lamp. The results of this simulations are shown in Figure 15.
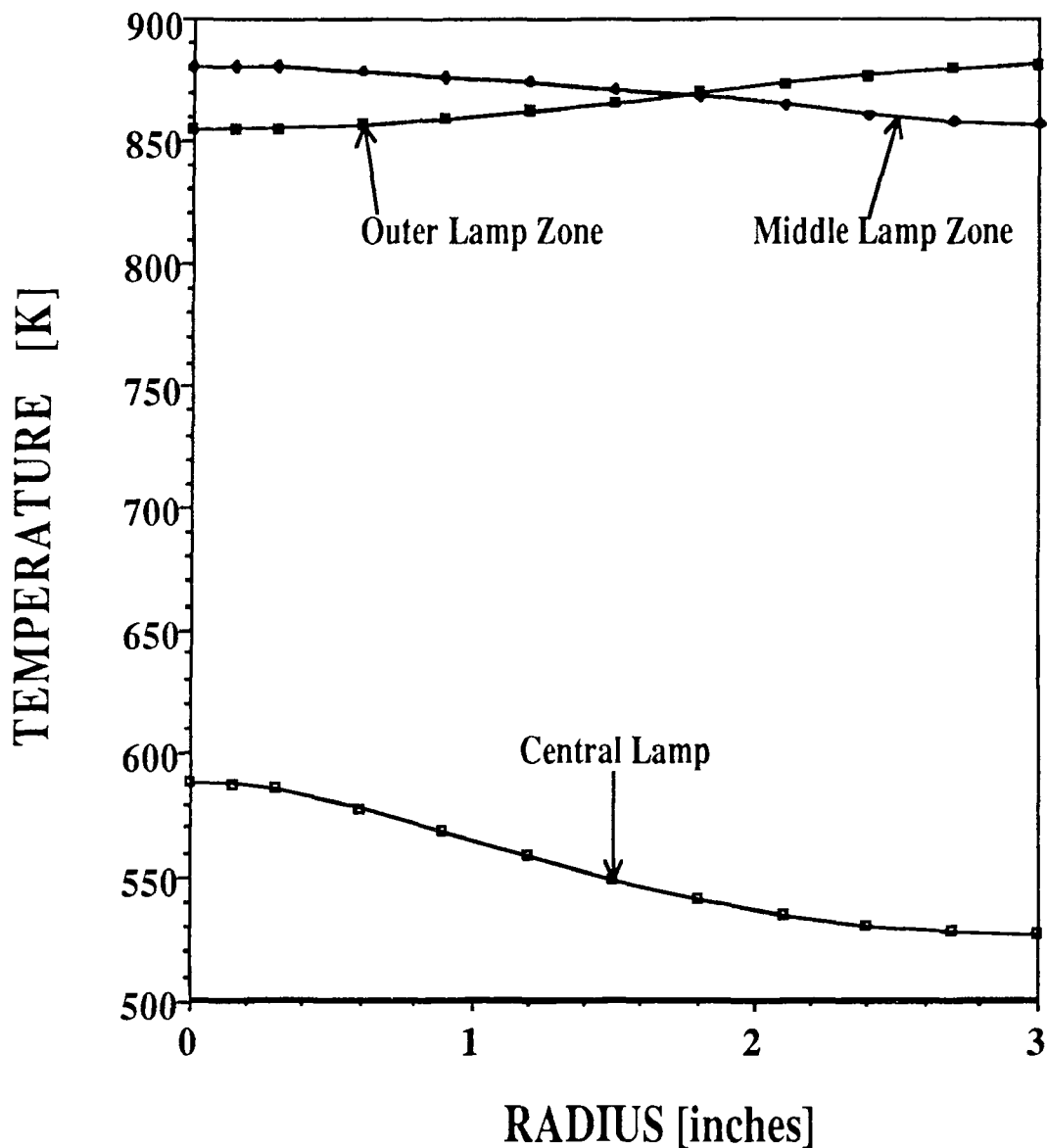

Figure 15. Radial temperature profiles resulting from heating the wafer by each zone of lamps separately. The effective emitting lamp power in each case is 225W.

The inspection of Figure 15 shows that the wafer temperature profile resulting from the heating by the middle lamp zone is of the similar shape to the profile resulting from heating by central lamp. This effect is due to the fact that the center of the wafer is being illuminated all 12 lamps of the middle zone, which has sufficiently small diameter to produce the commutative effect of "central heating". On the other hand the heating of the wafer by outer zone of lamps results in temperature profile with highest temperatures at the edge of the wafer due to comparatively large diameter of this lamp zone.
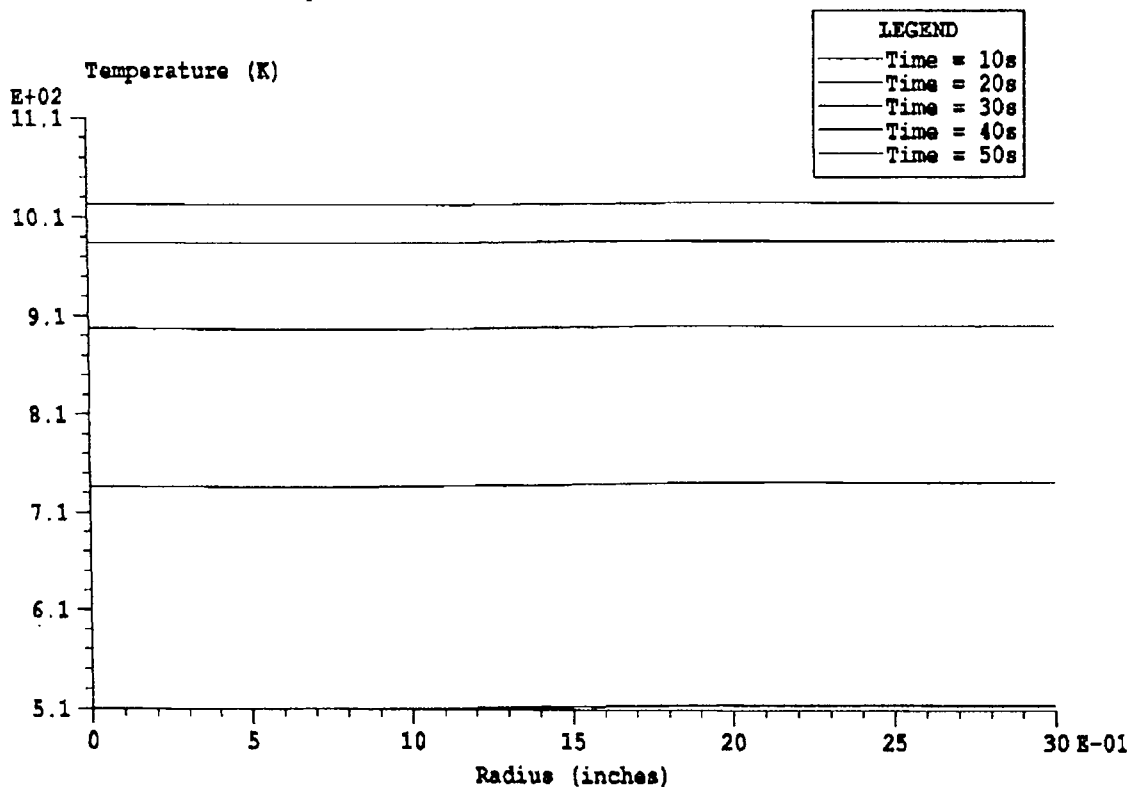
Figure 16. Radial temperature profile of the wafer resulting from heating by middle and outer lamp zones with equal effective emitting power of 225W per lamp.

Finally, it might be interesting to note, that the heating of the wafer with central lamp turned "off" and middle and outer lamp zones turned "on" with equal effective emitting power results in almost uniform temperature profile along the wafer radius as shown in Figure 16. The resulting steady-state non-uniformity in this case is less than 3° as illustrated in Figure 17.
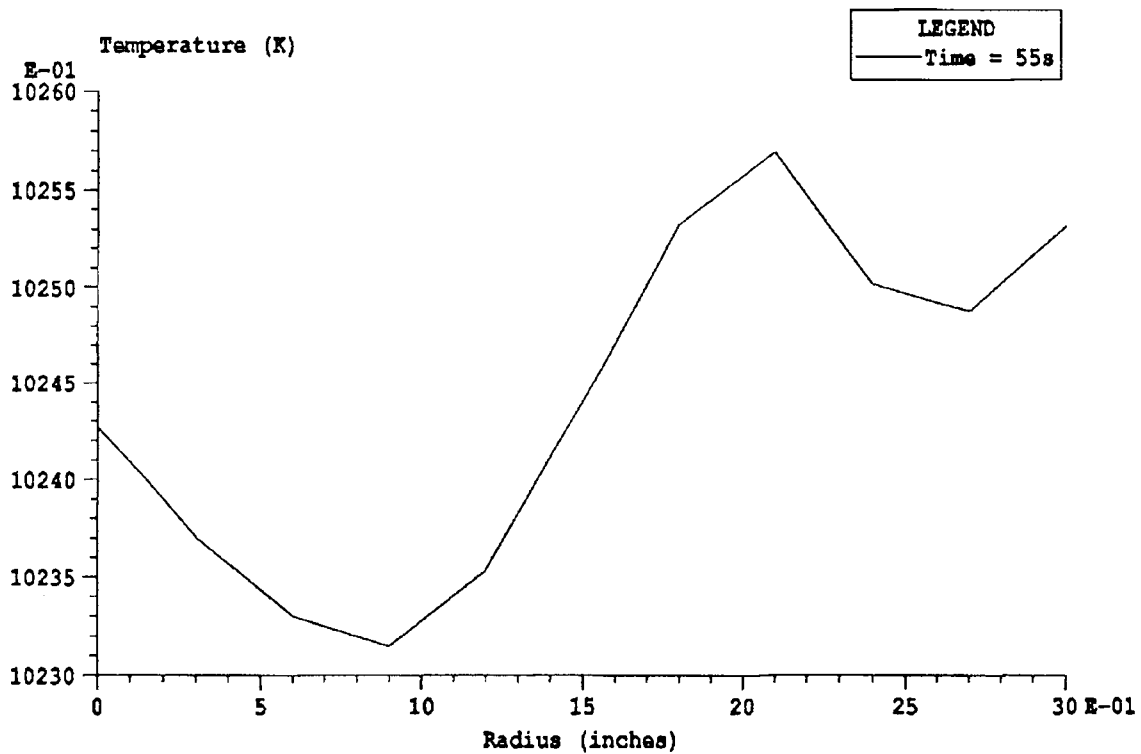

Figure 17. Steady-state non-uniformity resulting from heating by middle and outer lamp zones with equal effective emitting power of 225W per lamp.

5.1 Wafer Heating Along Prescribed Temperature Trajectory

In order to determine the emitting powers of the lamp zones required for uniform heating of the wafer according to the prescribed temperature trajectory the open-loop control algorithm was developed based on the simplified system model and optimization technique described in Section 5.1.

For the purpose of development of the open-loop control we divide the total period of time on which the prescribed trajectory is defined into a number of time intervals. Our objective is to find the effective emitting powers of each lamp zone $q_i^{em,lamps}$, within each time interval such that the deviation between prescribed and simulated temperature profiles will be minimized within this time interval. This will result in a set of effective lamp zone powers, one for each time step. This problem can be expressed as:

$$\min_{q_i^{em,lamps}} \left\{ F = \max_{t \in [t_i, t_{i+1}]} \sqrt{\sum_{j=1}^{N} \left(T^{r,j}(t) - T^j(t, T_{i-1}, q_i^{em,lamps}) \right)^2} \right\} \qquad (5\text{-}7)$$

where:

$q_i^{em,lamps}$ - is the vector of effective emitting powers of lamp zones in i-th time interval,

$T^r(t)$ - is the vector of prescribed temperatures,

N - is the number of points along the wafer radius at which temperature is prescribed (in our case N=11),

$T(t, T_{i-1}, q_i^{em, lamps})$ - is the vector of simulated temperatures.

The Eq. (5-7) was solved utilizing the MATLAB software package for the following temperature trajectory:

$$T^r(t) = 35 \cdot t + T_0 \qquad (5-8)$$

where T_0 - is the initial temperature of the wafer, assumed to be 300K.

The trajectory given by Eq. (5-8) corresponds to uniform heating of the wafer at the rate of 35°C per second. The resulting effective emitting powers of the lamps for the first 20 seconds are shown in Table 1.
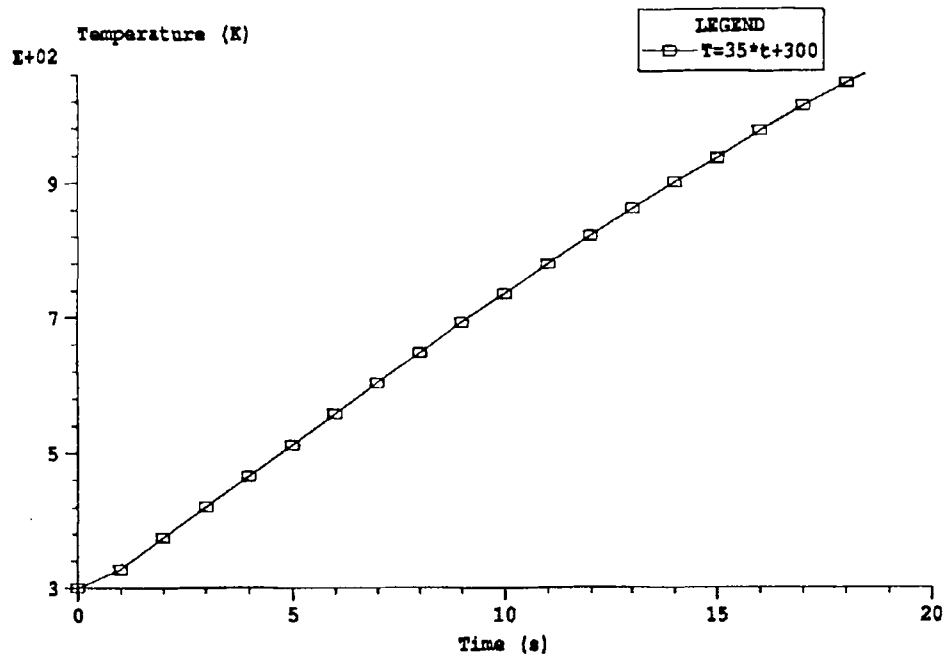
Figure 18. Simulation of heating along the prescribed trajectory given by Eq.(5-8).

Table 1. Calculated effective emitting powers for uniform wafer heating according to prescribed trajectory

Time (s)	Effective Power (W)		
	Center Lamp	Middle Zone Lamp	Outer Zone Lamp
0 - 5	54.2	433.0	362.7
5 - 10	63.4	441.1	378.4
10 - 15	71.7	467.8	408.5
15 - 20	81.3	530.8	465.5

The results of the finite-element simulation with lamp powers given in Table 1 are shown in Figure 18.

At each point in time the non-uniformity of the wafer temperature profile did not exceed 3°C as illustrated in Figure 19. Therefore, the open-loop control algorithm described in this Section provides effective means for the estimation of the lamp powers required for uniform heating of the wafer according to the prescribed temperature trajectory. The listing of the developed for open-loop control MATLAB function is given in the Appendix.
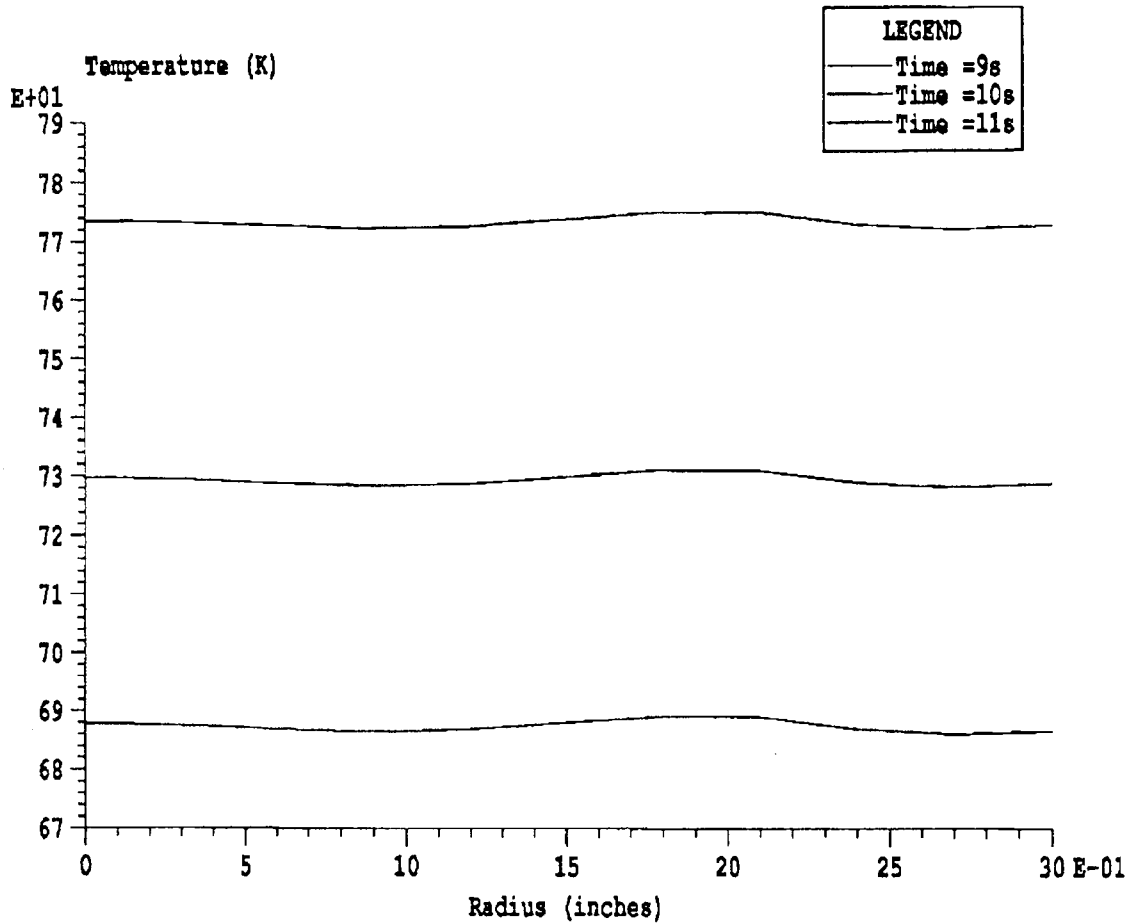
Figure 19. Uniformity of wafer temperature profile during the heating along the prescribed trajectory given by Eq.(5-8).

5.1 Effect of Thermocouple on Wafer Temperature Profile

One of the methods of measurement of wafer temperature profile during the RTP run is based on the utilization of instrumented wafers with a number thermocouples attached to wafer surface as illustrated in Figure 20. In the RTP system under consideration the K-type Nickel-Chrome thermocouples are utilized.
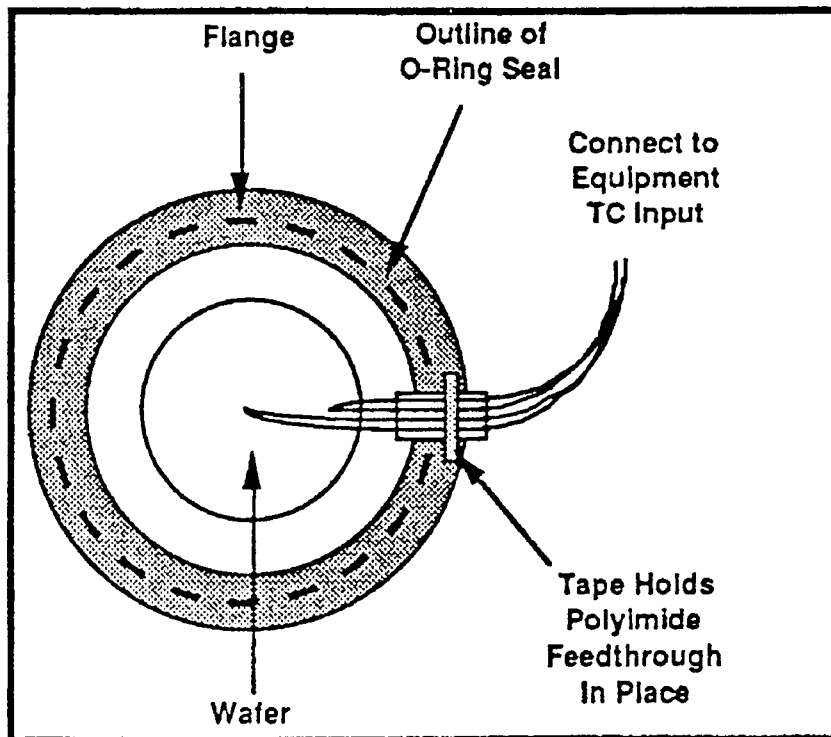
Figure 20. Instrumented wafer with attached thermocouples..

The thermocouples are attached to the wafer surface and their wiring are output from the process chamber through the water-cooled joint between the upper edge of the chamber wall and the quartz fixture. In this situation there is a conductive heat flow along the thermocouple wires due to the fact that one end of the thermocouple wiring is attached to the hot wafer surface and the other end is pressed to the water-cooled wall of the process chamber. The resulting heat flux will cause the disturbance in the wafer temperature profile in the proximity of the thermocouple and, therefore, the thermocouple reading will not reflect the correct wafer temperature. In

order to estimate this effect the model of thermocouple attached to the center of the wafer was incorporated into the finite element model of the RTP system as illustrated in Figure 21.
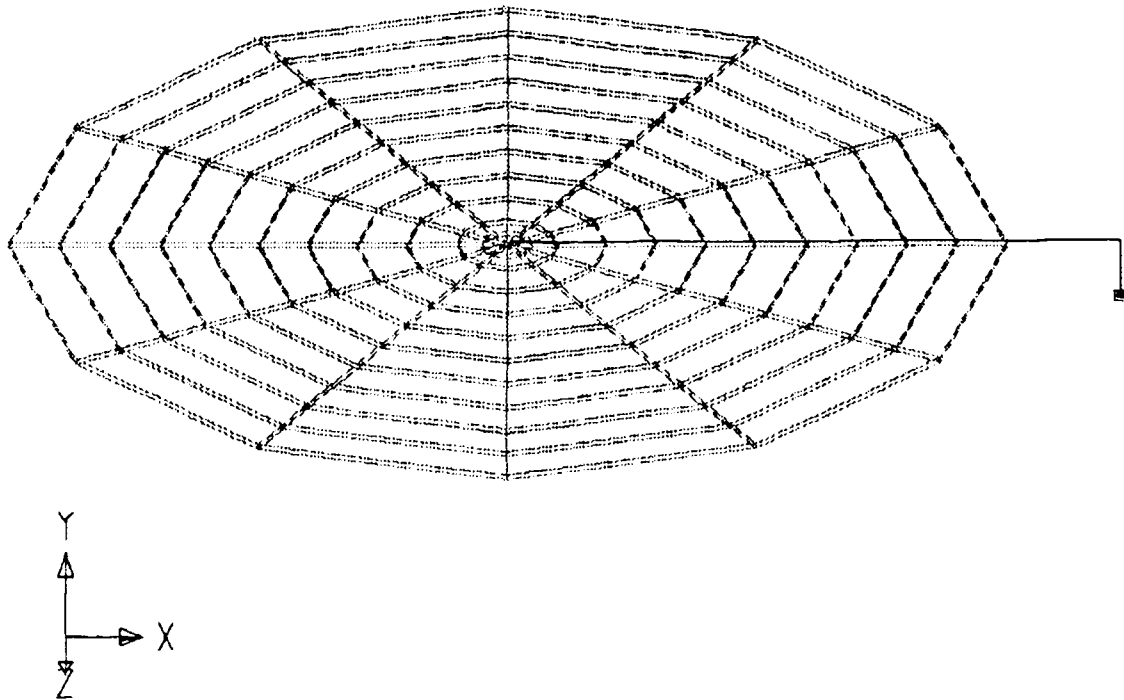
Figure 21. Modeling of thermocouple attached to the center of the wafer..

The thermocouple is modeled as ten one-dimensional "ROD" elements with the total length of 3.9" and crossectional area of 3.9×10^{-5} square inches, which corresponds to two thermocouple wires of 0.005" in diameter each. The thermal conductivity of the wires was assumed to be 0.046 cal/s K cm [3]. The resulting change of wafer temperature profile is approximately 0.1°C as illustrated in Figure 22. This disturbance in temperature profile is

in good agreement with suggested in [3] corrections of 0.013 to 0.168°C

for the heat loss due to conduction.
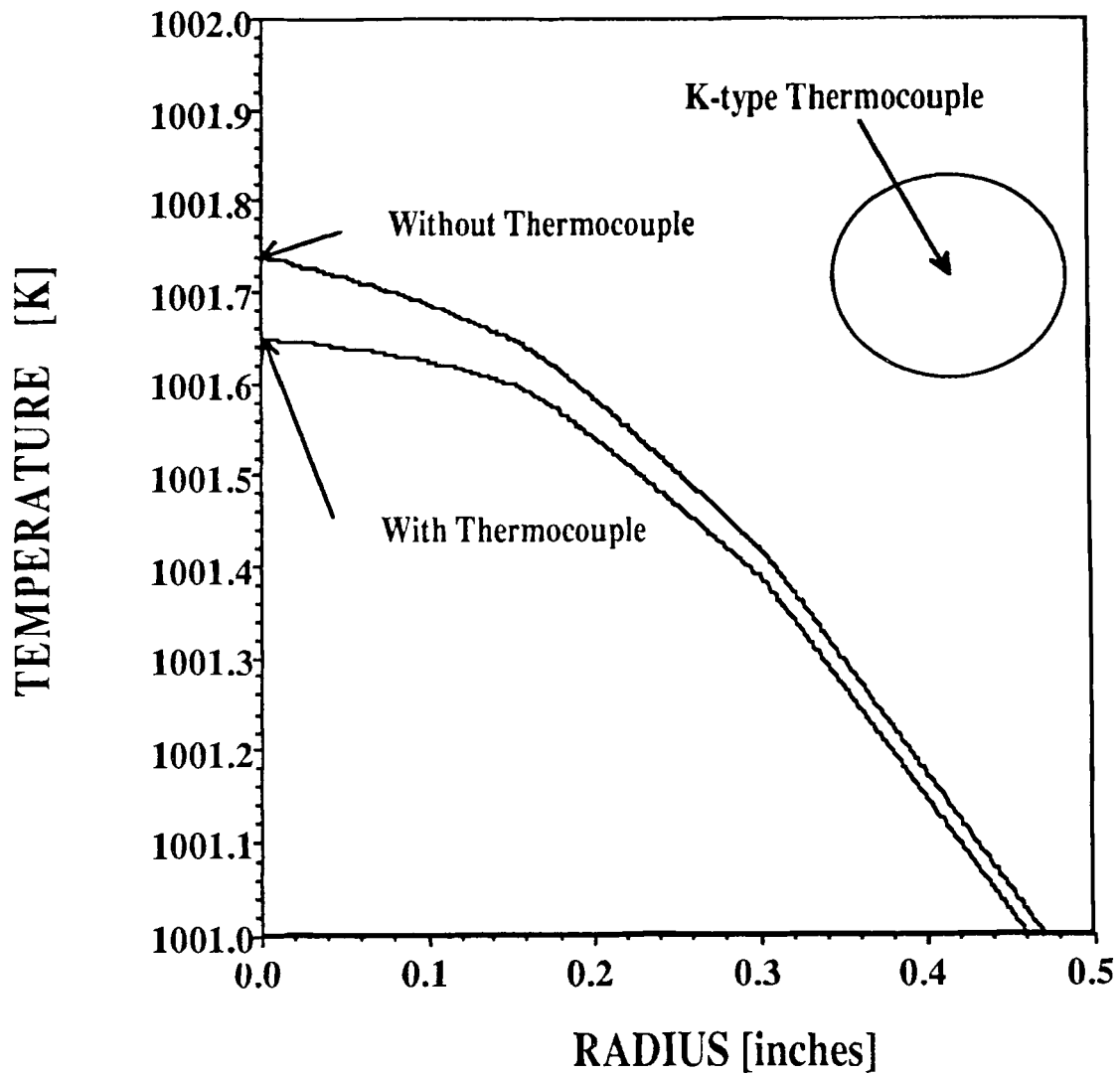
Figure 22. Simulated disturbance introduced in the wafer temperature profile by the presence of thermocouple.

CHAPTER 6

SUMMARY AND CONCLUSIONS

The finite element model of the RTP system was developed based on the MSC/NASTRAN software package. This model was calibrated against available experimental data in accordance with an algorithm developed in this thesis. The calibrated model was then utilized for analysis of the temperature profiles of the 6" silicon wafer for various combinations of the lamp powers.

Based on the developed model, the effects of each lamp zone on the wafer temperature profile was investigated. It was shown that the heating of the silicon wafer with equal effective radiant power from each lamp in three zones results in a temperature profile with the lowest temperatures at the edges of the wafer. For the effective radiant power from each lamp of 225W, the time constant of the process is of order of 30 seconds and the maximum temperature difference across the wafer is 60°K. When only the outer 2 lamp zones are operated the radial temperature distribution across the wafer varies less than 6°C.

The special emphasis in the present work was placed on the analysis of the requirements for uniform heating of the wafer along the prescribed temperature trajectory. In order to achieve this goal, the open-loop control algorithm was developed based on the simplified finite differences based

model of the RTP system. This algorithm allows the approximate variations in the lamp powers required for heating of the wafer along the prescribed temperature trajectory to be obtained. The algorithm was used to analyze temperature uniformity when the wafer heated at a rate of 35°C per second. It was shown that the non-uniformity of heating of the wafer along this trajectory can be less than 3°C.

The developed model was also utilized for the analysis of the change in the wafer temperature profile due to the heat loss through the thermocouple wiring attached to the wafer surface. It was shown that in case of K-type thermocouple with 0.005" diameter, the change in the wafer temperature profile in the proximity of the thermocouple is of the order of 0.1°C, which is in the good agreement with values published in the literature [3] for correction coefficients applied to thermocouple measurements.

It was also shown that view factors calculated by MSC/NASTRAN can be transformed to the form which can be utilized by real time control software for an accurate description of the system. The algorithm for realization of this transformation is presented in the thesis.

It should be pointed out that the present finite element model can be further refined in order to improve the accuracy of the simulated results. Among the possible improvements is the modeling of thermal conductivities of system components as a functions of temperature, since

the use of "effective" constant values of thermal conductivities introduces appreciable differences between simulated and actual transient behavior of the RTP system.

Finally, the accuracy of the model can be further improved by utilization of the developed calibration algorithm for more accurate estimation of model parameter based on the additional sets of experimental measurements as they become available.

APPENDIX

Program for Modeling of Semitransparent Quartz Window

The following program calculates the view factors needed for modeling of semitransparent quartz window according to the algorithm described in Chapter 3.

```c
# include <stdio.h>
# include <string.h>
# include <stdlib.h>
# include <math.h>
# include <ctype.h>
# define NE 351
# define NQ 20
# define TRANSMISSION 0.9
# define NL 37
# define A1 4.30696
# define A2 4.8276
# define A3 3.19944

FILE *fp, *fp1;

float
area[20]={A1,A2,A1,A3,A3,A1,A2,A1,A3,A3,A3,A3,A1,A2,A1,A3,A3,A
1,A2,A1};
char now,field[8],updated[10];
int LINE_N,ELEM_N,ITEM_N;

main()
{
int next_field();
int i,j;
float REFLECTION,K;
double item;
 fp=fopen("tes.dat","w");
 fp1=fopen("test.dat","r+");

LINE_N=0;
K=1.-TRANSMISSION;
while ((next_field()) != 0)  {
```

```
j=0; updated[8]=updated[7]=updated[0]=updated[9]=' ';
for(i=0;i<8;++i){
now=field[i];
if(now == '-') {updated[j]='e';j+=1;}
updated[j]=now;
j+=1; }
item=atof(updated);
```

```
/*    The transformation of view factor matrix  */
```

```
if(ITEM_N == 1) item=0.;
/*         From lamps to the wafer and the chamber    */
```

```
if((ITEM_N > (NL+1-LINE_N))&&(ITEM_N < (NE-NQ+1-LINE_N)))
item*=TRANSMISSION;
/*         From the chamber and the wafer on semitransparent quartz
window */
```

```
if((ITEM_N > (NE-NQ+1-LINE_N))) item*=K;
if((ITEM_N == 1)&&(LINE_N <= (NE-NQ))) fprintf(fp,"0\\"); else
/*         From quartz window on itself    */
```

```
if((ITEM_N == 1)&&(LINE_N > (NE-NQ)))
fprintf(fp,"%.5e\",TRANSMISSION*area[LINE_N-NE+NQ-1]);
else if((ITEM_N > 1)&&(ITEM_N <= (NE-LINE_N))&&(LINE_N >
(NE-NQ))) fprintf(fp,"0\\");
else if(ITEM_N > (NE-LINE_N)) fprintf(fp,"%.3e",item);
else fprintf(fp,"%.3e\",item);
}
fprintf(fp,"\n");
printf("K=%f\n",K);
fclose(fp);
fclose(fp1);
}
```

```
/*   This function reads the RADMXT cards deck field by field  */
```

```
int next_field ()
{
int i;
field[0]=getc(fp1);
```

```
if(ITEM_N > (NE-LINE_N)) {
while (isspace(field[0]) != 0) {field[0]=getc(fp1);
if (feof(fp1) != 0) { field[0]='F'; return(0);}}}
if((field[0]=='R')){
LINE_N+=1;
ELEM_N=2;
ITEM_N=0;
if(LINE_N == 1) fprintf(fp,"RADMTX\,%d\,",LINE_N);
else fprintf(fp,"\nRADMTX\,%d\,",LINE_N);
for (i=1; i < 17; ++i) field[0]=getc(fp1); } /* move reading point */
for (i=1; i < 8; ++i) field[i]=getc(fp1);
if(field[0]=='+'){
fprintf(fp,"%.8s\n%.8s\,",field,field);
for (i=0; i < 9; ++i) field[0]=getc(fp1);
for (i=0; i < 8; ++i) field[i]=getc(fp1);
ELEM_N=1;}
ELEM_N+=1;
ITEM_N+=1;
}
```

Program for Calculatin of Generalized Radiation Exchage Coefficients

The following MSC/NASTRAN input file provides the transformation of radiation exchange coefficients to the form appropriate for real time control algorithm.

```
ID MSC, PROB1    $
TIME 5
$
$  THE USER SHOULD SUPPLY RINGW MATRIX ON DMI CARDS.
$  THIS MATRIX DEFINES WHICH OF 11 RINGS OF THE WAFER
BELONGS TO USER DEFINED
$  BIGGER RING-MESH OF THE WAFER.
$
$  THE USER SHOULD SUPPLY RINGWSQ MATRIX ON DMI
CARDS.
$  THIS MATRIX DEFINES RATIO OF AREAS BETWEEN 11 RINGS
OF THE WAFER
$
SOL USERDMAP $ ,INCL=MSCOBJ $
```

```
COMPILE DMAP=USERDMAP,SOUIN=MSCSOU $
ALTER 2 $
$   INPUT OF A -MATRIX OF ELEMENTS AREAS,
$        FU - UPPER TRIANGULAR MATRIX OF RECALCULATED
VIEW FACTORS
$           WITH ADDED FIRST 6 ZERO RAWS
$        EA - DIAGONAL MATRIX OF ELEMENTS ABSORBIVITIES
$        RINGW - USER SUPPLIED MATRIX TO DEFINE THE
STRUCTURE OF CONTROL MODEL
$        RINGWSQ - USER SUPPLIED MATRIX TO DEFINE THE
STRUCTURE OF CONTROL MODEL
$
$   MATRIX RINGW SHOULD HAVE 11 RAWS (NUMBER OF
INITIALLY DEFINED RINGS ALONG THE
$   WAFER RADIUS BY THE MESH INTO FINITE ELEMENTS) AND
NUMBER OF COLUMNS
$   EQUAL TO DESIRED NUMBER OF RINGS ON THE WAFER.
$   I-TH RAW OF MATRIX RINGW DEFINES WHICH OF INITIAL
DEFINED RINGS BELONGS TO I-TH
$   USER DEFINED BIGGER RING, IF ELEMENT J BELONGS TO
RING I RINGW(I,J)=1, OTHERWISE - 0.
$   FOR EXAMPLE, IF USER WANTS TO HAVE 5 RINGS ON THE
WAFER (INSTEAD OF 11)
$   AND HE WANTS 1-ST,2-ND,3-RD RINGS OF EXISTED MESH TO
BE ONE (1-ST) NEW RING,
$   4-TH,5-TH - 2-ND NEW RING ,ETC
$   HE DEFINES RINNGW (11x5) MATRIX THE WAY SHOWN AT
THE END OF BULK DECK
$
DMIIN DMI,DMINDX/A,FU,EA,RINGW,RINGWSQ,,,,,/ $
MATPRN RINGW// $
TYPE PARM,,I,N,NOFR=37 $ NUMBER OF LAMPS IN FINITE
ELEMENT MODEL = 37
$
$   CREATING OF VIEW FACTOR SYMMETRIC MATRIX F
$
$   EXTRACTION OF FIRST 6 ZERO RAWS
MATGEN ,/UPARFU/6/357/6/351
PARTN FU,,UPARFU/TR1,FU1,TR2,TR3/1
$   SYMMETRIC F = FU (upper triangular) + FL (lower triangular)
TRNSP FU1/FL
```

```
ADD FL,FU1/F2
ADD F2,/F/0.5
$
$  CALCULATE RADIATION EXCHANGE COEFFICIENTS MATRIX
G = EA(A-F*(I-EA))-1*F
$
DIAGONAL A/IDENN/'SQUARE'/0. $ IDENTETY MATRIX
ADD IDENN,EA/X//-1.
MPYAD F,X,A/Y//-1
SOLVE Y,/YINV/3
MPYAD EA,YINV,/X1
MPYAD X1,F,/RE
$TRNSP G/RE
$
$  PARTITIONING G MATRIX INTO MATRICIES REPRESENTING
$  RLWT - RADIATION EXANGE COEFFICIENTS BETWEEN
WAFER TOP AND LAMPS,
$  RLWB - BETWEEN WAFER BOTTOM AND LAMPS,
$  RWTWT - BETWEEN WAFER TOP AND WAFER TOP,
$  RWTWB - BETWEEN WAFER BOTTOM AND WAFER TOP,
$  RWBWT - BETWEEN WAFER TOP AND WAFER BOTTOM,
$  RWBWB - BETWEEN WAFER BOTTOM AND WAFER BOTTOM
$
MATGEN ,/CP/6/351/0/37/132/30/132/20
MATGEN ,/RP/6/351/169/182
PARTN RE,CP,RP/RE11,RE21,RE12,RE22/1
$MATPRN RE11,RE21// $
MATGEN ,/CP1/6/264/132/132
MATGEN ,/RP1/6/169/37/132
PARTN RE11,CP1,RP1/RLWT,RWTWT,RLWB,RWTWB/1
$MATPRN RLWT,RWTWT// $ RESULT
MATGEN ,/RP2/6/182/0/30/132/20
PARTN RE21,CP1,RP2/RWBWT,RRR,RWBWB,RRR2/1
$
$  SUBDMAP OBRTOP -
$  RECOMPOSITION OF MATICIES OF EXCHANGE COEFFICIENTS
WITH WAFER TOP ELEMENTS,
$  IN ORDER TO OBTAIN CORRESPONDENCE BETWEEN WAFER
TOP AND WAFER BOTTOM ELEMENTS
$
CALL OBRTOP RLWT/LWT/NOFR
```

```
NOFR=132
CALL OBRTOP RWBWT/WBWT/NOFR
TRNSP RWTWB/RRWTWB
CALL OBRTOP RRWTWB/WTWB1/NOFR
TRNSP WTWB1/WTWB
TRNSP RWTWT/RRWTWT
CALL OBRTOP RRWTWT/WTWT1/NOFR
TRNSP WTWT1/WTWT
$
$    SINCE IN THE SIMPLIFIED MODEL THE WAFER DOES NOT
HAVE A WIDTH,
$    TOTAL RADIATION EXCHANGE COEFFICIENT ON THE
ELEMENT WITH TO SIDES IS
$    HALF OF THE SUM OF COEFFICIENTS ON BOTH SIDES
$
ADD LWT,RLWB/LW/
ADD5 RWBWB,WBWT,WTWB,WTWT,/W1W/
ADD W1W,/WW/0.5/0.5
$MATPRN LW,WW//
$
$    PARTITIONING MATRIX OF RADIOTION EXCHANGE COEFF.
BETWEEN LAMPS AND WAFER
$    INTO 3 MATRICES REPRESENTING COEFF. BETWEEN 3 RINGS
OF DISCRETE LAMPS
$    AND WAFER ELEMENTS
$    SUBDMAP SUMOFK -
$    GETTING THE SUM OF COEFFICIENTS FOR RADIATION
EXCHANGE BETWEEN LAMPS
$    AND WAFER ELEMENTS TO REPRESENT THE RADIATION
EXCHANGE BETWEEN WAFER
$    AND 3 RINGS OF LAMPS
$
TYPE PARM,,I,N,NUMOFL=12 $ NUMBER OF LAMPS IN THE 2-ND
RING
MATGEN ,/RR1/6/37/1/36
MATGEN ,/RR2/6/36/12/24
PARTN LW,,RR1/K1,K2A3,,/1
PARTN K2A3,,RR2/K2S,K3S,,/1
CALL SUMOFK K2S/K12/NUMOFL
ADD K12,/K2/0.0833333 $  ?
NUMOFL=24            $ NUMBER OF LAMPS IN THE 3-RD RING
```

```
CALL SUMOFK K3S/K13/NUMOFL
ADD K13,/K3/0.04166666 $  ?
$
$   CREATING THE MATRIX RASS
$   MATRIX RASS HAS 11 RAWS (NUMBER OF INITIALLY
DEFINED RINGS ALONG THE
$   WAFER RADIUS BY THE MESH INTO FINITE ELEMENTS) AND
132 COLUMNS (NUMBER
$   OF ELEMENTS IN THE WAFER)
$   I-TH RAW OF MATRIX RASS DEFINES WHICH OF WAFER
ELEMENT BELONGS TO I-TH
$   RING, IF ELEMENT J BELONGS TO RING I RASS(I,J)=1,
OTHERWISE - 0.
$
TYPE PARM,,I,N,NUM=1
TYPE PARM,,I,N,NUM11=1
TYPE PARM,,I,N,NUM111=1
MATGEN ,/NULMR/7/11/11/0/0
MATGEN ,/IDEN/1/11
DO WHILE (NUM<=12)
NUM111=11*NUM+11
NUM11=11*NUM
MATGEN ,/RPR/6/NUM111/NUM11/11
MERGE NULMR,IDEN,,,,RPR/NULMMR/1
EQUIVX NULMMR/NULMR/ALWAYS
NUM=NUM+1
ENDDO
MATGEN ,/RPR1/6/143/11/132
PARTN NULMR,,RPR1/NULMT,RASS,,/1
$
$   CALCULATION OF RADIATION EXCHANGE COEFFICIENTS
MATRICIES
$   RESLW/1,2,3/ - BETWEEN 1-ST,2-ND,3-RD RING OF LAMPS
RESPECTIVELY
$               AND 11 WAFER RINGS,
$   RESWW - BETWEEN WAFER RINGS
$
MPYAD K1,RASS,/RESLW1
MPYAD K2,RASS,/RESLW2
MPYAD K3,RASS,/RESLW3
MPYAD WW,RASS,/PRRES
```

```
MPYAD RASS,PRRES,/RESW1W/1
ADD RESW1W,/RESWW/0.08333333
$
$   CALCULATION OF RESULTED RADIATION EXANGE
COEFFICIENT MATRICIES
$   NLW/1,2,3/ BETWEEN USER DEFINED RINGS ON THE WAFER
AND 1,2,3 RINGS OF LAMPS
$   NWW - BETWEEN USER DEFINED RINGS ON THE WAFER AND
THEMSELVES
$   PRINTING THE RESULTED MATRICIES
$
MPYAD RESLW1,RINGW,/NLW1
MPYAD RESLW2,RINGW,/NLW2
MPYAD RESLW3,RINGW,/NLW3
MATPRN NLW1// $
MATPRN NLW2,NLW3// $
MPYAD RESWW,RINGWSQ,/PRRES1
MPYAD RINGW,PRRES1,/NWW/1
MATPRN NWW// $
$
$   SUBDMAP SUMOFK
$
COMPILE SUBDMAP=SUMOFK
SUBDMAP SUMOFK KS/K/NUMOFL
MATGEN ,/IDR/6/NUMOFL/0/NUMOFL
TRNSP IDR/IDDR
MPYAD IDDR,KS,/K
RETURN
END
$
$   SUBDMAP OBRTOP
$
COMPILE SUBDMAP=OBRTOP
SUBDMAP OBRTOP WT/R2/NOFR
TYPE PARM,,I,N,KK=1
TYPE PARM,,I,N,II=0
TYPE PARM,,I,N,I121=-1
TYPE PARM,,I,N,I110K1=-1
TYPE PARM,,I,N,I11K1=-1
TYPE PARM,,I,N,I111=-1
MATGEN ,/NULM/7/NOFR/131/0/0
```

```
MATGEN ,/UP/6/132/0/131
DO WHILE (II<=11)
I121=II+121
MATMOD WT,,,,,/COL1,/1/I121
I111=11*II
MATGEN ,/UP1/6/132/I111/1
MERGE NULM,,COL1,,UP1,/NULMM/1
PARTN NULMM,UP,/NUL1,,NULMM1,/1
EQUIVX NULMM1/NULM/ALWAYS
$
DO WHILE (KK<=10)
I110K1=10*II-KK+11
MATMOD WT,,,,,/COL2,/1/I110K1
I11K1=11*II+KK
MATGEN ,/UP2/6/132/I11K1/1
MERGE NULM,,COL2,,UP2,/NULM2/1
PARTN NULM2,UP,/NUL2,,NULMM2,/1
EQUIVX NULMM2/NULM/ALWAYS
KK=KK+1
ENDDO
KK=1
II=II+1
ENDDO
MERGE NUL2,,NULMM2,,UP,/R2/1
RETURN
END
CEND          $ END OF USERDMAP
$
TITLE = CALCULATION OF RADIATION EXCHANGE
COEFFICIENTS
ECHO = NONE
BEGIN BULK
$ INPUT A
$
DMI,A,0,6,1,0,,351,351
$      ..............
DMI,A,351,351,4.30696
$
$ INPUT FU
$
DMI,FU,0,2,1,0,,357,351
```

```
$       ..............
+504409,0.0,0.0,0
$
$ INPUT EA
$
DMI,EA,0,6,1,0,,351,351
$       ..............
DMI,EA,351,351,4.30696
$
$ INPUT OF RINGW AND RINGWSQ
$       ...............
$
ENDDATA
```

Main Input File of RTP Model

The following represents the main input file to MSC/NASTRAN. This file contains the information about the RTP system needed for finite element modeling.

```
ID MSC, ALL LAMPS ON
$
$     MAXIMUM CPU TIME ALLOWED FOR THE JOB
$
TIME 333 $ UNITS ARE MINUTES
$
$     THE THERMAL ANALYZER PORTION OF MSC/NASTRAN IS
TO BE USED
$
APP HEAT
$
$     THE NON-LINEAR TRANSIENT SOLUTION ALGORITHM IS
TO BE USED
$
SOL 89
$
CEND $ END OF EXECUTIVE CONTROL DECK
$
$*******
$     END OF EXECUTIVE CONTROL  ...  START CASE CONTROL
```

```
$*******
$
TITLE=        TRANSIENT PROBLEM
ECHO = NONE
$
$     SPECIFY THE SUPERELEMENTS TO BE RUN
$     THIS CARD IS REQUIRED AND SPECIFIES ALL
$     FOR THIS MODEL THERE IS BUT A SINGLE SUPERELEMENT
WHICH
$              ENCOMPASSES THE ENTIRE MODEL
SEALL=ALL
$
DLOAD=800
$
TEMP(ESTI) = 7
$
TSTEP = 500
$
$     SELECT THE TEMPERATURE SET DEFINING THE
TEMPERATURE VECTOR AT
$     TIME = O.
$
IC  = 600
$
$
$     SELECT THE OUTPUT DESIRED (TEMPERATURES AND
LOADS)
$
SET 1 = 13 THRU 24
$SET 1 = 1 THRU 35,1500 THRU 1525
SET 2 = 501 THRU 620,1001 THRU 1133
OUTPUT
THERMAL = 1
$OLOAD=1
$
$FLUX=2
$
$*******
$     END CASE CONTROL ... START BULK DATA
$
BEGIN BULK $ ENDS CASECONTROL DECK
```

```
$
PARAM,POST,0
$    DEFINE THE TIME STEP
TSTEP,500,1000,.01,100,,,,,+TST
+TST,,450,0.1,10
TEMPD,600,300.
$
$    DEFINE THE LOAD
$
DLOAD,800,1.0,1.0,700,1.0,710,1.0,712,+D
+D,1.0,713
TLOAD2,700,400,,,0.,1.+6,0.,0.,+TL
+TL,0.,0.
$
TLOAD1,710,300,,,10
TLOAD1,712,304,,,14
TLOAD1,713,306,,,16
$
$    TEMPERATURE ON OUTTER RING
$
TABLED2,10,0.,,,,,,,+TA
+TA,0.,300.,2.,2000.,1000.,2000.,ENDT
$
$    TEMPERATURE OF CENTER LAMP
$
TABLED2,14,0.,,,,,,,+TA4
+TA4,0.,300.,2.,1673.,1000.,1673.,ENDT
$
$    TEMPERATURE ON INNER RING
$
TABLED2,16,0.,,,,,,,+TA6
+TA6,0.,300.,2.,2000.,1000.,2000.,ENDT
$
$    IN THIS PROBLEM INCHES, CALORIES AND DEGREES
KELVIN ARE USED.
$
$    DEFINE GRID POINTS
$
$  TOP OF THE CHAMBER
$
$  BOTTOM OF THE CHAMBER
```

```
$
$       ...........................
GRID   833              3.25368 0.0     1.73529
$
$       DEFINE ELEMENTS OF THE CHAMBER
$
CQUAD4 301    101    711    833    732    610
$       ...........................
CTRIA3  390    101    722    821    831
$
$       RADIOMETRIC PROPERTIES OF THE CHAMBER
PHBDY,102,,,0.01,0.1
$
CHBDY,801,102,AREA4,711,610,732,833,100
$       .......................
CHBDY,890,102,AREA3,821,831,722,,100
$
$              WAFER
$ WAFER GRIDS
$
GRID,1,,3.000000,9.560000,0.000000
$       .......................
GRID,506,,0.129904,9.585000,0.075000
$
$   WAFER BOUNDARY ELEMENTS
$
CHBDY,501,2,AREA4,36,37,14,13,50
$       .......................
CHBDY,1122,22,AREA3,12,11,495,,60
$
PHBDY,2,,,,.5,.6
PHBDY,22,,,,.5,.6
$
$   WAFER FINITE ELEMENTS
$
CHEXA  1    1    1    25    26    2    13    36    +
+    37    14
$       ...........................
CPENTA 132    1    495    11    12    506    23    24
$
$       DEFINE PROPERTY CARD
```

```
$
PSOLID,1,100
PSHELL,101,55,0.001
$
$       DEFINE MATERIAL THERMAL CONDUCTIVITY AND
THERMAL CAPACITY
$
MAT4,100,1.15,14.
MAT4,55,10.              $  property of chamber
$
$       QUARTZ GRIDS AND ELEMENTS
$
$
GRID,1500,,0.0,9.67,0.0
$       ..................
GRID,1521,,3.253680,10.17,1.735290
$
$
CHBDY,1250,12,AREA3,610,1500,620,,10
$       ..................
CHBDY,1259,12,AREA3,701,1500,711,,10
$
$       CONVECTIVE QUARTZ BOUNDARY
$
CHBDY,1226,12,AREA3,1505,1502,1503,,,+CON1
+CON1,2000,2000,2000
$       ........................
CHBDY,1225,12,AREA3,1503,1502,1521,,,+CON
+CON,2000,2000,2000
$
GRID,2000,,0.,-1.,0.    $  AIR
$
$
PSOLID,11,33
MAT4,33,0.075,9.3734
PHBDY,12,120,,0.189,0.189
MAT4,120,0.0001
$
CELAS2,1700,1.+6,2000,1
SLOAD,400,2000,300.+6
$
```

```
$
CPENTA  1200   11     1500   620    610    1502   1505   1503
$       ...........................
CPENTA  1209   11     1500   610    711    1502   1503   1521
$
$
$   DEFINE RADIANT SOURCE
$
$
GRID,900,,0.000000,10.73000,0.000000
GRID,901,,2.250000,12.300,0.000000
$       ...............
GRID,912,,1.948560,12.300,-1.125000
GRID,950,,4.000000,11.42000,0.000000
$       ...............
GRID,973,,3.863700,11.42000,-1.035280
$
$
CHBDY,400,4,POINT,900,,,,50,+R1
+R1,,,,,0.,-1.,0.
$       ...............
CHBDY,473,5,POINT,973,,,,50,+R73
+R73,,,,,0.,-1.,0.
$
$
TEMPD,7,800.
$
PARAM,SIGMA,8.7376-12
PARAM,MAXIT,30
PARAM,EPSHT,0.00001
$VIEW,50,1,1,3,3
$VIEW,60,1,1,2,2
$
PHBDY,4,,0.785398,1.
PHBDY,5,,0.3848451,1.
PHBDY,6,,0.3848451,1.
$
$   DEFINE PRESCRIBED TEMPERATURE
$
CELAS2,1600,1.+6,900,1
SLOAD,304,900,1.+6
```

```
$        .....................
CELAS2,1542,1.+6,833,1
SLOAD,400,833,300.+6
$
$  DEFINE VIEW FACTOR MATRIX
$
RADMTX,1,0.,0.0,0.0,0.0,0.0,0.0,0.0,+500000
$        .....................
RADMTX,351,3.87626
RADLST    400    401    402    403    404    405    406
407+1000000
$        .....................
+1000042   1253   1254   1255   1256   1257   1258   1259
$
$*******
$    END OF BULK DATA DECK
$
ENDDATA
```

MATLAB functions for Open Loop Control Algorithm

```
function  [F]=funn1(coef,Tn,num)

%Function FUNN1 computes the maximum norm of
%temperature  deviations

t0=num-5;  tf=num;
x0=[Tn;coef1];
%Function DIF represents the system of differential
%equations discrabing the simplified model of RTP

[t,x]=ode45('dif',t0,tf,x0);
[nt,mt]=size(t);
[nx,mx]=size(x);
for
j=1:nt,
```

```
tfn(j)=35*t(j)+300;
end
for
i=1:nt,
s(i)=norm(x(i,1:11)-[tfn(i)  tfn(i)  tfn(i)  tfn(i)  tfn(i)  tfn(i)
tfn(i)
tfn(i)  tfn(i)  tfn(i)  tfn(i)]);
end
F=max(s);

function  [Tl1,Tl2,Tl3,f,yy,yyy]=lamptemp(TT,coef,time,op)
cf=coef;
%Function lamptemp searches for minimum of temperature
%diviations at each time interval.

Tn=TT;
yy=[0 0 0 0 0 0 0 0 0 0 0];
yyy=yy;
   for i=1:time,
j=5*i;
x=fmins('funn1',cf,op,[],Tn',j);
[t,y]=ode45('dif',j-5,j,[Tn  x']);
f(i)=funn1(x,Tn',j);
[nt,mt]=size(t);
Tn=y(nt,1:11);
if i < 8,  yy=[yy;y(:,1:11)];
else yyy=[yyy;y(:,1:11)];      end
cf=x;
Tl1(i)=x(1);
Tl2(i)=x(2);
Tl3(i)=x(3);
   end
save b:resf2.mat Tl1  Tl2  Tl3  f  yy  yyy
```

REFERENCES

1. S.R. Wilson, R.B. Gregory and W.M. Paulson. "An Overview and Comparison of Rapid Thermal Processing Equipment: A User Viewpoint" in *Rapid Thermal Processing*, Symposia Proceedings of Materials Research Society, 52 (181), Pittsburgh (1986)

2. Electronic Imaging Center of NJIT. Proposal for ARPA Contract "Multi-Wavelength Imaging Pyrometry for Semiconductor Process Monitoring and Control", (1992)

3. *Manual on the Use of Thermocouples in Temperature Measurement*, ASTM Special Technical Publication 470B, Baltimore, MD (1992)

4. H.A. Lord. "Thermal and Stress Analysis of Semiconductor Wafers in a Rapid Thermal Processing Oven", *IEEE Trans. Semicond. Manufact.*, 1(3):105-114. August (1988)

5. W.H. Booth (Editor.), "MSC/NASTRAN Handbook for Thermal Analysis", MSC/NASTRAN Version 65, MacNeal-Schwendler Corp., Los Angeles, (1986)

6. J.R. Welty. *Engineering Heat Transfer*, John Wiley & Sons Inc., (1978)

7. Courant R., "Variational Method for the Solution of Problems of Equilibrium and Vibrations", *Bulletin of American Mathematical Society*, Vol. 49, (1943)

8. S.S. Rao, *The Finite Element Method in Engineering*, Pergamon Press, (1982)

9. R.H. MacNeal (Editor), *The NASTRAN Theoretical Manual*, MacNeal-Schwendler Corp., Los Angeles, (1972)

10. *MSC/NASTRAN Programmer's Manual*, MSC/NASTRAN Version 64, MacNeal-Schwendler Corp., Los Angeles, (1986)

11. S.A. Norman, "Wafer Temperature Control in Rapid Thermal Processing", Ph.D. Dissertation, Dept. of Electrical Engineering, Stanford University, (1992)

12. C.E.Third, F.Weinberg and L.Young *Mathematical Model of Internal Temperature Profile of GaAs during Rapid Thermal Annealing, J. Appl. Phys.* 69(12), August (1991)